

Development of Novel *Bryophyllum Pinnatum* Chitosan Loaded Nanoparticle for Invitro Antioxidant, Antimicrobial Anticancer Studies

^{1,3}Ahmad Muazu Shehu* and ^{2,3}Erkay Özgör

¹Department of Bioengineering, Faculty of Engineering, Cyprus International University, Nicosia, North Cyprus, Mersin 10, Turkey.

²Department of Molecular Biology and Genetics, Faculty of Arts and Sciences, Cyprus International University, Nicosia, North Cyprus, Mersin 10, Turkey.
North Cyprus, Mersin 10, Turkey.

³Department of Microbiology, Bayero University, Kano-Nigeria.
shehu_muazu@yahoo.com*

(Received on 11th March 2024, accepted in revised form 27th March 2025)

Summary: Cancer, characterized by uncontrolled cell proliferation, remains a leading cause of mortality worldwide. Conventional therapies often face limitations, including severe side effects, drug resistance, and non-specificity. Nanotechnology offers a promising alternative, and *Bryophyllum pinnatum*, known for its antioxidant, antimicrobial, and anticancer properties, provides a sustainable source of bioactive compounds for nanoparticle-based therapeutics. *Bryophyllum pinnatum*-loaded chitosan nanoparticles (BPCNPnp) were synthesized using the ionic gelation method and characterized for their physicochemical and biological properties. Gas chromatography-mass spectrometry (GC-MS) analysis identified eight bioactive compounds in the extract, including alpha-linolenic acid, oleic acid, and ethyl palmitate. The nanoparticles exhibited a particle size of 116.7 nm, a zeta potential of +28.84 mV, and a polydispersity index (PDI) of 0.25, indicating enhanced stability and uniformity. Compared to conventional chitosan nanoparticles (CNPnp), BPCNPnp demonstrated superior DPPH radical scavenging capacity, with an IC₅₀ value of 4.26 mg/mL, closely matching ascorbic acid (IC₅₀ = 4.00 mg/mL), while CNPnp showed an IC₅₀ of 5.32 mg/mL. The nanoparticles exhibited significant antimicrobial activity against Gram-negative bacteria, with inhibition zones up to 17.33 ± 1.52 mm for *Klebsiella pneumoniae* and 15.66 ± 1.15 mm for *Escherichia coli* at 8000 µg/mL. Antifungal activity was observed against *Aspergillus niger*, with an inhibition zone of 15.70 ± 0.57 mm. Cytotoxicity and MTT assays revealed dose- and time-dependent antiproliferative effects on MDA-MB-231 breast cancer cells, reducing cell viability by 66% at 24 h and 42% at 48 h at 300 µg/mL, compared to 76% and 66% reductions for CNPnp. These findings demonstrate the superior stability, antioxidant capacity, antimicrobial efficacy, and anticancer potential of BPCNPnp, making it a promising nanopatform for addressing challenges in oxidative stress, antimicrobial resistance, and cancer treatment.

Keywords: BPCNPnp, *Bryophyllum pinnatum* loaded chitosan nanoparticle, CNPnp, chitosan nanoparticles, BP, *Bryophyllum pinnatum*, Nanotechnology, Anticancer, Antioxidant, Antimicrobial.

Introduction

Cancer, characterized by the uncontrolled proliferation of cells that can metastasize to other parts of the body, remains a leading cause of mortality worldwide. Most cancer-related deaths are attributed to metastasis. Breast cancer, the second leading cause of death among females globally, accounts for approximately 24% of cancer-related fatalities [1]. Conventional cancer treatments, including chemotherapy, surgery, and targeted therapies, often face limitations such as side effects, toxicity, non-selective action, and resistance, ultimately reducing patients' life expectancy [2]. These challenges necessitate the exploration of innovative technologies to overcome the limitations of conventional therapies, improve patient outcomes,

and extend life expectancy [3]. Furthermore, recent studies have highlighted the significance of the tumor microenvironment and immune evasion mechanisms in cancer progression, paving the way for novel therapeutic strategies [4].

Nanotechnology has emerged as a groundbreaking approach in cancer research and therapy. This technology spans multiple domains, including medicine, imaging, drug delivery, and nanostructure design, typically within a size range of 1–100 nm [5]. Nanotechnology has gained rapid traction in various scientific and industrial fields, including food, cosmetics, healthcare, mechanical, and chemical industries, showcasing its vast potential

*To whom all correspondence should be addressed.

[6]. Nanoparticles have demonstrated great promise in overcoming limitations associated with conventional drug delivery, including poor bioavailability, rapid degradation, and non-specific toxicity [7]. Specifically, nanoparticles can enhance drug solubility, improve therapeutic efficacy, and facilitate targeted delivery to cancer cells, thereby minimizing systemic side effects [8]. Additionally, recent advancements in the development of stimuli-responsive nanoparticles, such as pH-sensitive and temperature-sensitive systems, have further enhanced the precision and efficacy of nanotechnology-based cancer therapies [9].

Recent developments have also seen the emergence of personalized mRNA-based cancer vaccines. Companies like BioNTech and Moderna, known for their COVID-19 vaccines, are now focusing on cancer vaccines that train the immune system to recognize and attack tumor-specific proteins [10]. These vaccines are currently undergoing clinical trials and show promise in reducing cancer recurrence. For instance, Moderna's mRNA-4359 vaccine has demonstrated the potential to stop tumor growth and prevent new diseases in early trials [11]. Additionally, innovative treatments such as AngioDynamics' Canonize have received FDA approval for prostate cancer treatment. This technology uses irreversible electroporation to target and destroy cancer cells while preserving surrounding healthy tissue, offering a less invasive option with potentially fewer side effects [12]. These developments underscore the dynamic and evolving landscape of cancer research and treatment, with nanotechnology playing a pivotal role in advancing therapeutic strategies [13].

Bryophyllum pinnatum, also known as the "Miracle Leaf," "Love Plant," and "Life Plant," is a succulent herb belonging to the family Crassulaceae. It is primarily cultivated in regions such as Africa, Madagascar, China, India, and Australia [14]. Traditionally, this plant has been used to treat urinary tract problems and kidney stones. Its leaves are known for their therapeutic properties and have been used to treat microbial infections, asthma, and ulcers [15]. Studies have demonstrated its antimicrobial, anti-ulcer, anti-diabetic, and anti-mutagenic activities [16]. Key phytochemicals isolated from *Bryophyllum pinnatum* include flavonoid glycosides, quercetin, bufadienolides, and lipids, as well as bioactive compounds such as bufotoxin A, B, and C, caffeine, and protocatechuic acid, which contribute to its antioxidant and cytotoxic properties [17]. Recent investigations have focused on its potential role in modulating oxidative stress and inflammatory

pathways, which are critical in cancer progression [18].

Chitosan, a cationic polysaccharide derived from chitin (a major component of arthropod exoskeletons and fungal cell walls), has gained recognition for its non-toxic, biocompatible, biodegradable, and low-allergenic properties [19]. These qualities make chitosan an excellent candidate for synthesizing nanoparticles to address the challenges of conventional cancer treatments [20]. Chitosan nanoparticles exhibit notable antibacterial activity due to their ability to bind to negatively charged residues on bacterial cell walls, leading to membrane disruption and bacterial death [21]. Additionally, chitosan possesses antifungal properties that are effective against yeast and spore-forming microorganisms [22]. Chitosan nanoparticles also display significant potential in cancer therapy due to their ability to facilitate the controlled and sustained release of therapeutic agents, enhance cellular uptake, and induce apoptosis in cancer cells [23]. Moreover, functionalizing chitosan nanoparticles with targeting ligands or encapsulating hydrophobic drugs has further improved their therapeutic index and specificity [24].

Recent advancements have demonstrated the synergistic potential of combining natural bioactive compounds with nanotechnology to create more effective therapeutic agents. For instance, plant-derived nanoparticles, including those synthesized using *Bryophyllum pinnatum*, have shown enhanced stability, bioavailability, and therapeutic efficacy compared to traditional formulations [25]. These nanoparticles are particularly valuable in targeting oxidative stress and inflammation, which are crucial in cancer progression [26]. Moreover, the incorporation of *Bryophyllum pinnatum* extracts into chitosan nanoparticles not only leverages the plant's intrinsic therapeutic properties but also addresses limitations such as poor water solubility and rapid degradation of phytochemicals [27].

The ionic relation method has emerged as a preferred technique for synthesizing chitosan nanoparticles due to its simplicity, cost-effectiveness, and ability to preserve the bioactivity of loaded compounds [28]. This method involves the electrostatic interaction between the positively charged chitosan and a polyanion, leading to nanoparticle formation. The resulting nanoparticles exhibit high encapsulation efficiency, controlled drug release, and enhanced cellular uptake, making them ideal for biomedical applications [29]. The

nanoparticles were characterized through various spectroscopic imaging and scanning techniques. The antibacterial activity of CNPNP, conventional chitosan nanoparticles (CNP), and *Bryophyllum pinnatum* methanolic extract was evaluated against seven pathogenic microorganisms, including three Gram-negative bacteria (*Escherichia coli*, *Klebsiella pneumoniae*, and *Salmonella typhi*), two Gram-positive bacteria (*Staphylococcus aureus* and *Streptococcus pneumoniae*), and two fungi (*Aspergillus Flavus* and *Aspergillus niger*). A hydrogen peroxide scavenging assay was employed to assess the in vitro free radical scavenging activity of the nanoparticles and the extract [30]. MTT and cytotoxicity assays were performed to evaluate cell viability and proliferation of breast cancer cells, highlighting the potential of the synthesized nanoparticles as a novel therapeutic agent for cancer.

This study focuses on synthesizing *Bryophyllum pinnatum*-loaded chitosan nanoparticles (CNP) using the ionic relation method treatment.

Objectives of the Study

- i. Collection and authentication of *Bryophyllum pinnatum*.
- ii. Synthesis of *Bryophyllum pinnatum*-loaded chitosan nanoparticles (BPCNP).
- iii. Characterization of *Bryophyllum pinnatum*-loaded chitosan nanoparticles (BPCNP).
- iv. Assessment of the antioxidant activity of *Bryophyllum pinnatum*, BPCNP, and CNP.
- v. Evaluation of the antimicrobial activity of *Bryophyllum pinnatum*, BPCNP, and CNP against pathogenic microorganisms.
- vi. Evaluation of the anticancer activities of BPCNP and CNP against breast cancer cell lines (MDA-MB-231), including:
 - a. Cytotoxicity Study using Trypan Blue Exclusion Assay
 - b. Methyl-Thiazolyl Tetrazolium (MTT) Assay

Experimental

Material

Chitosan (medium molecular weight = 150,000; degree of deacetylation 90%) obtained from Sigma-Aldrich (USA) 1-diphenyl-2-picrylhydrazyl (DPPH) purchased from Sigma-Aldrich (USA) butylated hydroxytoluene (BHT) sourced from Sigma-Aldrich (USA) dried leaves of *Bryophyllum*

pinnatum collected locally from wudil local Government kano state, ethanol analytical grade obtained from Merck (Germany) sodium tripolyphosphate (TPP) reagent grade purchased from Merck (Germany) hydrochloric acid (HCl) analytical grade sourced from Merck (Germany) sodium hydroxide (NaOH) analytical grade obtained from Merck (Germany) glacial acetic acid reagent grade purchased from Merck (Germany) nutrient broth microbiological grade obtained from HiMedia (India) sodium chloride (NaCl) reagent grade purchased from Merck (Germany) hexane analytical grade sourced from Merck (Germany) barium chloride (BaCl₂) analytical grade purchased from Merck (Germany) sulfuric acid (H₂SO₄) analytical grade sourced from Merck (Germany) and sodium sulfate (Na₂SO₄) analytical grade purchased from Merck (Germany). Distilled water was obtained from Cyprus International University (CIU) and used throughout the entire study.

Methods

Plant collection and identification

Fresh leaves of *Bryophyllum pinnatum* were collected from the Wudil Local Government Area of Kano State, Nigeria (latitude: 11.794242, longitude: 8.839032). The specimen was authenticated by a botanist from the Plant Biology Department, Bayero University, Kano, and assigned voucher number BUKHAN 0014, which was deposited in the university herbarium. The leaves were washed with deionized water, shade-dried, and ground into a coarse powder using a mortar and pestle.

Preparation of Extract

The extract of *Bryophyllum pinnatum* was prepared using a modified method from Alqatani *et al.* [31]. Fifty-five grams of the powdered leaves were dissolved in 330 mL of aqueous ethanol (1:6 ratio) and left to stand for 3 hours with occasional stirring. The mixture was then filtered through Whatman filter paper, and the filtrate was concentrated using a rotary evaporator at 45°C to yield a greenish-dark viscous extract. This extract was stored at 5°C for further use.

Synthesis of *Bryophyllum pinnatum* Chitosan Nanoparticles

The ionic gelation method was used to synthesize *Bryophyllum pinnatum* chitosan nanoparticles (BPCNP) and free chitosan nanoparticles (CNP), as described by Isbilan &

Vural with modifications [32]. Chitosan (0.05 g) was dissolved in 50 mL of 1% (v/v) acetic acid and stirred continuously at 800 rpm for 8 hours to form a homogeneous solution. A 10 mg/mL solution of *Bryophyllum pinnatum* extract was prepared separately. Sodium tripolyphosphate (TPP) solution (0.05%) was also prepared in distilled water and stirred at 700–800 rpm for 3 hours. The pH of the chitosan solution was adjusted to 4.6 using NaOH.

To synthesize nanoparticles, the TPP solution was added dropwise to the chitosan solution under continuous stirring to facilitate cross-linking. Afterwards, the *Bryophyllum pinnatum* extract solution was added dropwise and stirred for 30 minutes to ensure proper incorporation. The resulting suspension was filtered using a 0.45- μ m syringe filter, centrifuged at 11,000 rpm for 25 minutes, and freeze-dried to obtain BPCNPnp. CNPnp was synthesized similarly, but without adding the *Bryophyllum pinnatum* extract.

Gas Chromatography-Mass Spectrometry (GC-MS)

The ethanol extract of *Bryophyllum pinnatum* was subjected to GC-MS analysis using a GC-MS QP 2010 Plus system equipped with a TRB-5MS column. A 1 μ L sample was injected in split-less mode, with helium as the carrier gas at a flow rate of 1 mL/min. The initial column temperature was set at 50°C, which was increased at a rate of 7°C/min until reaching 70°C. The electron impact ionization mode was operated at 70 eV, and spectra were scanned over a mass-to-charge ratio (*m/z*) range of 25–1000.

Characterization

UV-Vis Spectroscopy: The absorbance spectra of the nanoparticles were measured between 200 and 800 nm using a Shimadzu UV-2450 spectrophotometer.

FTIR Spectroscopy: Functional groups were identified using a Fourier Transform Infrared Spectrometer (Shimadzu model) within the range of 4000–500 cm^{-1} .

Zeta potential analysis: A zeta potential analyzer (Microtrac Instruments, model: Nanotrac Wave) was used to assess the zeta potential of both the unloaded and loaded hydrogel membranes at 25 °C

Scanning electron microscopy (SEM) The synthesized hydrogel morphology was examined using a scanning electron microscope. It also

provides structural details, especially if

Energy Dispersive X-ray Spectroscopy (EDS): The elemental composition of the nanoparticles was analyzed using a Phenom ProX EDS. Samples were prepared on carbon tape and analyzed without further coating to maintain their elemental integrity.

Antioxidant Assays

DPPH radical scavenging activity was assessed to evaluate the antioxidant capacity of BPCNPnp, CNPnp, *Bryophyllum pinnatum* extract, and ascorbic acid (positive control). Serial dilutions (5–160 $\mu\text{g/mL}$) of the samples were prepared, and the absorbance was measured at 513 nm using a 64-well microplate reader after 30 minutes of incubation [34]. The percentage inhibition was calculated using the following equation:

The percentage inhibition was calculated using the following equation:

$$\text{Inhibition (\%)} = \frac{A_{\text{control}} - A_{\text{sample}}}{A_{\text{control}}} \times 100$$

where A_{control} is the absorbance of the control and A_{sample} is the absorbance of the sample.

Antimicrobial Activity

The antimicrobial activity of *Bryophyllum pinnatum* extract, BPCNPnp, and CNPnp was tested against five bacterial strains—three gram-negative (*Salmonella typhi*, *Escherichia coli*, *Klebsiella pneumoniae*) and two gram-positive (*Staphylococcus aureus*, *Streptococcus pneumoniae*)—as well as two fungal strains (*Aspergillus flavus*, *Aspergillus niger*). The disc diffusion method, as described by Ogbonna et al. [34], was employed to assess antimicrobial efficacy.

Preparation of Bacterial Suspension

Each bacterial strain was serially diluted with nutrient broth to prepare a bacterial suspension. The suspensions were incubated at 37°C for 24 hours, following the standard method outlined by McFarland for bacterial suspension preparation.

Preparation of Agar Plates

Mueller-Hinton agar plates were prepared by dissolving a specific quantity of powdered media in distilled water and autoclaving at 121°C for 15 minutes at 15 psi. The sterile media was aseptically poured into 60mm Petri dishes and allowed to

solidify.

Application of Bryophyllum pinnatumnanoparticle and extract.

After the agar plates had dried, 200 µl of the bacterial suspension was evenly spread onto the surface of the agar. Sterile 6 mm discs were loaded with 30 µl of the prepared BPCNPnp, CNPnp, or *Bryophyllum pinnatum* extract. For control, 30 µl of ciprofloxacin (500 µg/disc) and ketoconazole (200 µg/disc) were used as positive controls, while dimethyl sulfoxide (DMSO) served as a negative control [35].

Incubation and Measurement

The agar plates were incubated at 37°C for 24 hours. The zones of inhibition were observed and measured in millimetres (mm) to assess the antimicrobial activity of each extract and nanoparticle formulation. Each experiment was performed in triplicates to ensure reproducibility. Statistical analysis of the zone diameters was performed using SPSS software, with the Duncan test used to evaluate significant differences between the treatment groups.

Cytotoxicity Study using Trypan Blue Exclusion Assay

This study assessed the antiproliferative and cytotoxic effects of *chitosan* nanoparticles (CNPnp) and *Bryophyllum pinnatum*-loaded *chitosan* nanoparticles (BPCNPnp) on *MDA-MB-231* breast cancer cell lines over various time points and concentrations. *MDA-MB-231* breast cancer cells were cultured in *DMEM* supplemented with 10% fetal bovine serum, 100 U/mL penicillin, and 100 µg/mL streptomycin. Cells were incubated with BPCNPnp and CNPnp at concentrations ranging from 10–300 µg/mL for 24, 48, and 72 hours [36].

Trypan Blue Exclusion: The total number of cells (viable + non-viable) was counted, and the viable cells were recorded [37].

The normalized cell number in percentage was calculated using the following formulae

$$\text{Normalized cell Number (\%)} = \frac{\text{Number of viable cells}}{\text{Total number of cells}} \times 100$$

Methyl-Thiazolyl Tetrazolium (MTT) Assay

The proliferation of *MDA-MB-231* cells was

evaluated using the colourimetric 3-(4,5-dimethylthiazol-2-yl)-2,5-diphenyltetrazolium bromide (MTT) assay as previously outlined by Mani & Swargiary [38]. Cells were seeded at a density of 3×10^4 /mL and left to adhere overnight before being treated with BPCNPnp and CNPnp extracts. Absorbance measurements were taken at 490 nm using a multi-well plate reader (ELx800, Biotek Instruments). All experiments were conducted in triplicate [38, 39].

The percentage viability was calculated using the following equation:

$$(\%) \text{ viability} = \frac{\text{Absorbance of sample}}{\text{Absorbance of control}} \times 100$$

Statistical Analysis

Statistical analysis was performed using SPSS (Statistical Package for the Social Sciences). One-way analysis of variance (ANOVA) was conducted, followed by Duncan's test to determine significant differences between the observed values. All results were considered statistically significant at $p < 0.05$.

Results and Discussion

Synthesis and Characterization of BPCNPnp and CNPnp

BPCNPnp and CNPnp were synthesized using the ionic gelation method with modifications. The bioactive components of the *Bryophyllum pinnatum* (Bp) aqueous ethanolic extract were analyzed using Gas Chromatography-Mass Spectrometry (GC-MS), and the results are shown in Fig. 1. The intensity of peaks against retention times. A total of eight compounds were identified, each characterized by distinct peaks, intensities, and retention times. Among these, five compounds—Alpha-linolenic acid, oleic acid [40], 1,2-Benzenedicarboxylic acid [41], Hexadecanoic acid ethyl ester (CAS), Ethyl palmitate [42], Cholest-5-en-3-ol 3.beta [43], and 3-[2-(1,3-Diolan-2-yl)ethyl]but-2-enolide [44]—are known for their biological activities. However, compounds like Silane, trimethyl[(3. beta.)-stigmast-5-en-3-yl]oxy- and Thunbergol 2,7,11-Cyclotetradecatrien-1-ol lack documented biological activities in the literature. Additionally, 6-Perfluorohexyl-1-trimethylsiloxy-1-cyclohexene, a newly identified compound, has yet to be investigated for its biological properties. Analysis of bioactive compounds using Gas Chromatography-Mass Spectrometry (GC-MS) from *Bryophyllum*

pinnatum(Bp) were identified and analyzed. Eight compounds were identified, among which Alpha-linolenic acid, oleic acid, 1,2-Benzenedicarboxylic acid, Hexadecanoic acid ethyl ester (CAS), Ethyl palmitate, Cholest-5-en-3-ol 3.beta, and 3-[2-(1,3-Diolan-2-yl)ethyl]but-2-enolide are known for their biological activities. These compounds contribute to the therapeutic potential of Bp. Interestingly, the newly identified compound 6-Perfluorohexyl-1-trimethylsiloxy-1-cyclohexene presents an opportunity for further investigation to determine its biological properties. Zeta sizer measurements indicated that BPCNPnp had a size of 116.7 nm and a Zeta potential of 28.84 mV (Fig. 2A&B). In contrast, CNPnp exhibited a size of 95.6 nm and a Zeta potential of 24.86 mV (Figs 2C&D). These parameters are key indicators of nanoparticle size and stability, with a lower Zeta potential value often indicating instability, which may lead to cluster formation and precipitation [45]. BPCNPnp demonstrated a unimodal size distribution with slight distortion, likely due to particle aggregation. Its size distribution of 116.7 nm is consistent with similar chitosan-based nanoparticles, which typically range from 32.7 to 1100 ± 20 nm [46]. The recorded polydispersity index (PDI) for BPCNPnp was 0.25, suggesting a relatively uniform nanoparticle solution, as corroborated by Fig. 2. CNPnp exhibited a unimodal distribution with a size of 95.6 nm (Fig. 2C), suitable for drug delivery and biomedical applications. However, its PDI value of 0.38 suggests a broader size distribution, indicating potential heterogeneity. Optimization of the synthesis process may be required to improve uniformity. Comparative analysis revealed that BPCNPnp had a higher Zeta potential (28.84 mV) than CNPnp (24.86 mV), indicating enhanced stability and reduced aggregation [47]. This difference may be attributed to the encapsulation of Bp into CNPnp [48]. The Zeta sizer measurements revealed that BPCNPnp had a size of 116.7 nm and a Zeta potential of 28.84 mV, whereas CNPnp had a size of 95.6 nm and a Zeta potential of 24.86 mV. The higher Zeta potential of BPCNPnp indicates enhanced stability and reduced aggregation compared to CNPnp. The size distribution of BPCNPnp is consistent with similar chitosan-based nanoparticles, and its polydispersity index (PDI) of 0.25 suggests a relatively uniform nanoparticle solution. In contrast, the PDI value of 0.38 for CNPnp indicates potential heterogeneity and may require optimization of the synthesis process to improve uniformity. UV-visible spectroscopy was employed to identify distinct absorption patterns across various wavelengths. Both CNPnp and BPCNPnp exhibited consistent absorption within the 200–250 nm range (Fig. 3), consistent with previous

studies [49]. Both CNPnp and BPCNPnp exhibited consistent absorption within the 200–250 nm range, aligning with previous studies. This consistent absorption indicates that the nanoparticles maintain their structural integrity and can be effectively utilized in drug delivery and biomedical applications. Fourier-transform infrared spectroscopy (FTIR) provided insights into the functional groups present in the nanoparticles. For CNPnp, peaks were observed at 1047, 1408, 1563, 1719, 1995, and 3777 cm^{-1} , corresponding to functional groups such as CO-O-CO stretching and NH stretching. In BPCNPnp, broader peaks at 853, 1578, 1418, 1991, 2985, and 3788 cm^{-1} suggested the presence of C=C aromatic and P-C organophosphate groups (Fig. 8). FTIR analysis provided insights into the functional groups present in the nanoparticles. CNPnp exhibited peaks corresponding to CO-O-CO stretching and NH stretching, while BPCNPnp showed broader peaks indicating the presence of C=C aromatic and P-C organophosphate groups. These functional groups play a crucial role in the biological activities and stability of the nanoparticles. Scanning Electron Microscopy (SEM) revealed that CNPnp particles formed polyhydric and aggregated clusters (Fig. 5B), while BPCNPnp exhibited rod-like structures and organized clusters, likely influenced by encapsulation (Fig. 5A). SEM analysis revealed that CNPnp particles formed polyhydric and aggregated clusters, whereas BPCNPnp exhibited rod-like structures and organized clusters. The encapsulation of Bp into CNPnp likely influenced the structural organization of BPCNPnp, contributing to its enhanced stability and reduced aggregation. Elemental composition analysis via Energy Dispersive X-ray Spectroscopy (EDS) revealed similarities in elements like sodium, phosphorus, and magnesium for both nanoparticles, with carbon uniquely present in BPCNPnp, contributing to its higher molecular weight Fig.6 Energy Dispersive X-ray Spectroscopy (EDS) revealed similarities in elements like sodium, phosphorus, and magnesium for both nanoparticles. However, the presence of carbon uniquely in BPCNPnp contributed to its higher molecular weight. This difference in elemental composition may influence the biological activities and therapeutic potential of the nanoparticles. The synthesis and characterization of BPCNPnp and CNPnp demonstrated their potential for biomedical applications. BPCNPnp, with its enhanced stability, uniform size distribution, and presence of bioactive compounds, presents a promising candidate for drug delivery and therapeutic.

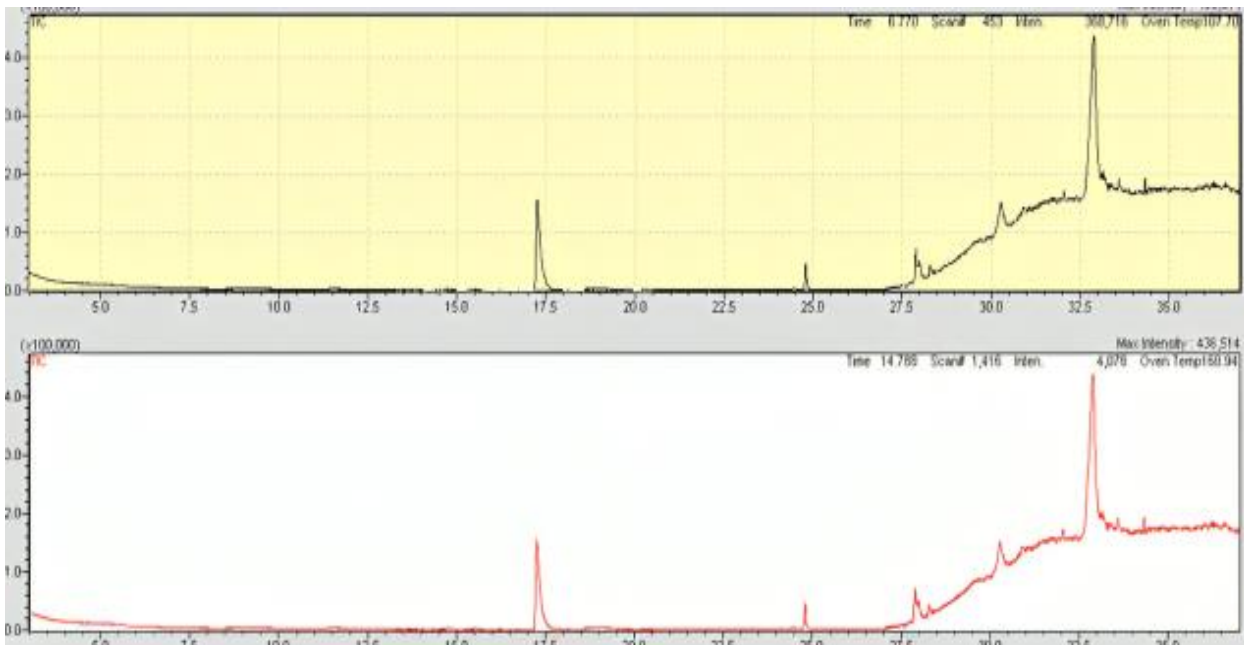


Fig. 1: Peaks identified in the GC-MS analysis of the aqueous-ethanolic extract of *Bryophyllum pinnatum*.

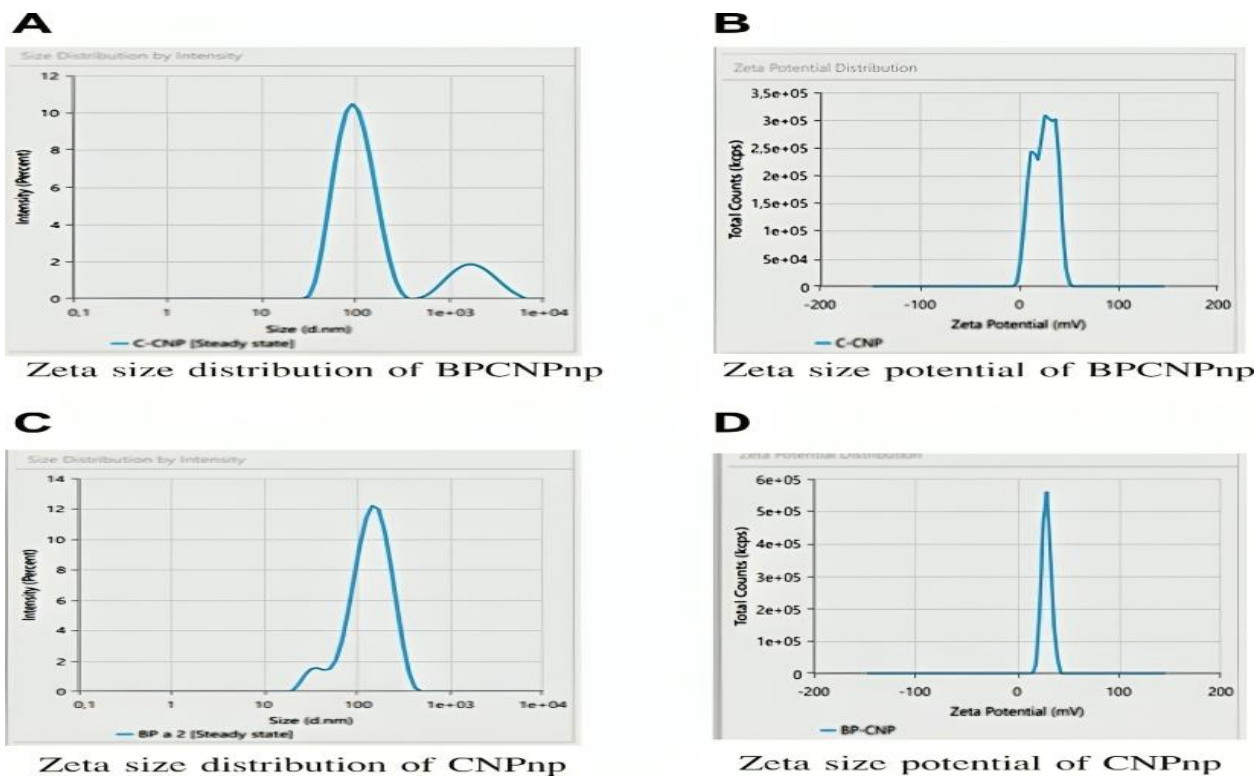


Fig. 2: Zeta size and potential distribution of BPCNPnp and CNPnp.

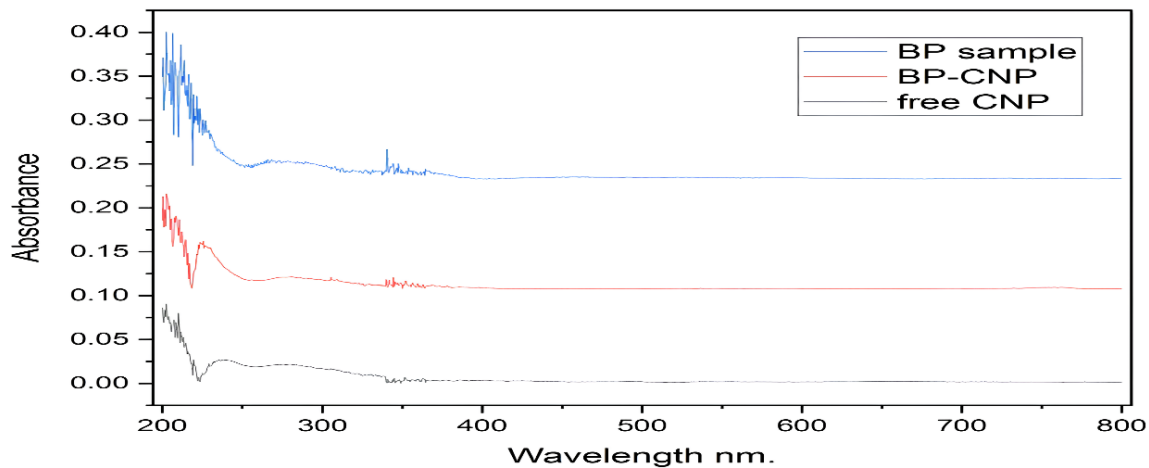


Fig. 3: UV-visible spectra of *Bryophyllum pinnatum* (BP), BPCNPnp, and CNPnp.

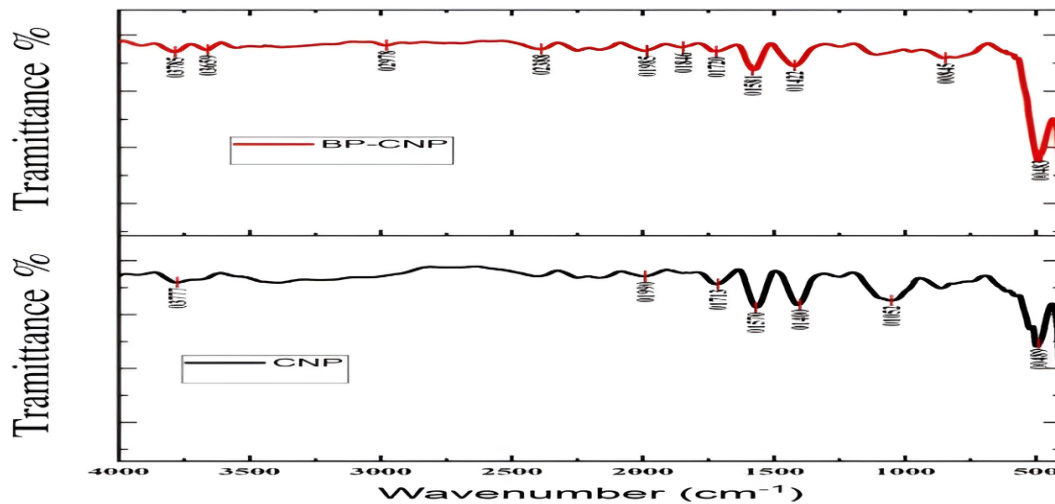


Fig. 4: FTIR spectra of BPCNPnp and CNPnp.

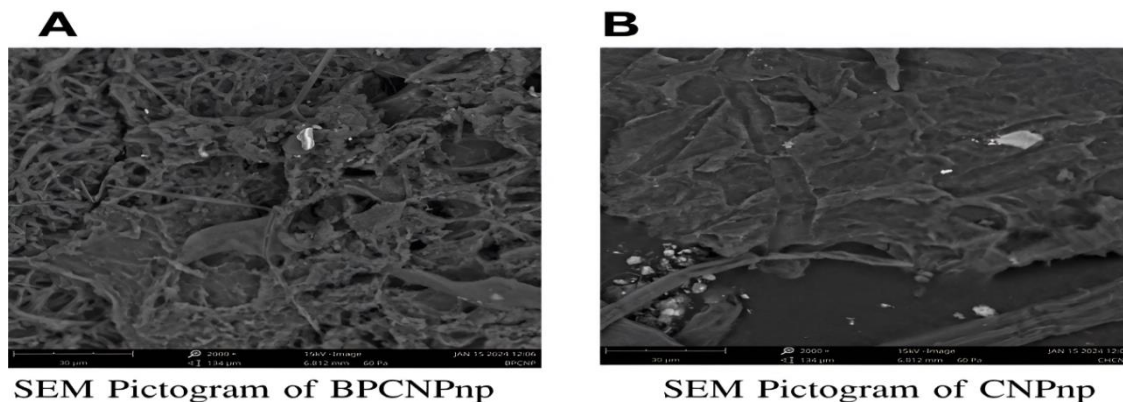


Fig. 5: SEM micrographs of (A) BPCNPnp and (B) CNPnp, highlighting the surface morphology and structural characteristics of the nanoparticles.

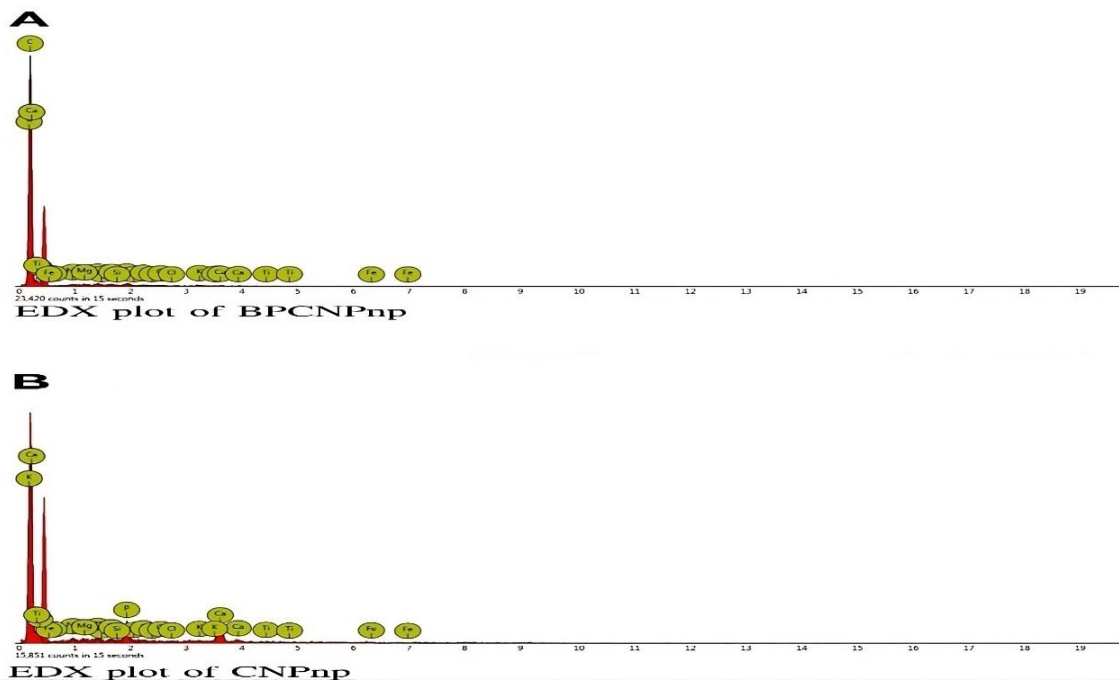


Fig. 6: EDX spectra of BPCNPnp and CNPnp showing the elemental composition of the nanoparticles.

Antioxidant Activity

Bryophyllum pinnatum-loaded chitosan nanoparticles (BPCNPnp) were synthesized and evaluated for their antioxidant activity. The encapsulation of Bp within chitosan nanoparticles is expected to improve its therapeutic efficacy by protecting the bioactive compounds from degradation and ensuring sustained release. The antioxidant potential of BPCNPnp was assessed using the DPPH radical scavenging assay, a widely used method for determining the ability of a compound to donate hydrogen and neutralize free radicals. The findings provide insights into the enhanced antioxidant activity of BPCNPnp compared to unencapsulated Bp extract and non-loaded chitosan nanoparticles (CNPnp), demonstrating the potential of nanocarriers in improving the functionality of natural antioxidants. This section explores the antioxidant activity of BPCNPnp, comparing its efficacy to ascorbic acid, Bp extract, and CNPnp. The impact of encapsulation on antioxidant performance is also discussed, highlighting the potential advantages of nanoparticle-based delivery systems in biomedical application. BPCNPnp demonstrated remarkable antioxidant activity, ranking second only to ascorbic acid. The encapsulation process likely enhanced the stability and controlled release of antioxidants from the chitosan nanoparticles, contributing to improved scavenging activity. Previous research has

highlighted the potential of chitosan-based nanocarriers in increasing the bioavailability and efficacy of antioxidant compounds [50].

The DPPH proton scavenging assay was performed on CNPnp, BPCNPnp, and *Bryophyllum pinnatum*(Bp) aqueous-ethanolic extract across a concentration range of 5–160 µg/mL, as shown in Fig. 7. A reduction in the DPPH deep purple color to yellow phenylhydrazine was visually observed for ascorbic acid, BPCNPnp, Bp extract, and CNPnp, with varying intensities. Comparative analysis revealed that ascorbic acid exhibited the highest DPPH scavenging activity, followed by BPCNPnp, the Bp ethanolic extract, and CNPnp in descending order. This result highlights the enhanced antioxidant potential of BPCNPnp compared to the Bp extract.

The antioxidant activities of ascorbic acid, BPCNPnp, CNPnp, and the crude ethanolic extract of Bp indicate differences in their abilities to scavenge free radicals. Ascorbic acid, a well-known antioxidant, showed the highest DPPH radical scavenging activity, consistent with previous studies emphasizing its exceptional antioxidant capabilities due to efficient electron donation and free radical neutralization [51]. BPCNPnp displayed significant antioxidant activity, ranking just below ascorbic acid. The enhanced performance of BPCNPnp is likely due to encapsulation, which stabilizes and controls the release of antioxidants. This result aligns with earlier

findings suggesting that chitosan-based nanocarriers can improve the bioavailability and effectiveness of antioxidant compounds [52]. CNPnp, lacking encapsulation, exhibited antioxidant activity, though it was less pronounced compared to BPCNPnp. The difference may stem from the protective effect of encapsulation, which shields antioxidants from environmental degradation and ensures a controlled release. Previous studies have attributed the antioxidant activity of chitosan and its derivatives to their ability to scavenge free radicals [53].

The crude ethanolic extract of Bp demonstrated antioxidant activity but ranked lower than both the chitosan-encapsulated and non-encapsulated nanoparticles. The extract's efficacy can be attributed to its diverse phytochemical composition, although factors such as extraction methods and solvent selection influence its overall antioxidant potential [54].

The observed variations in DPPH antioxidant activity among ascorbic acid, BPCNPnp,

CNPnp, and the Bp extract underscore the critical role of formulation and encapsulation techniques in optimizing the antioxidant capacity of bioactive compounds. The results support the hypothesis that encapsulating Bp within BPCNPnp enhances its antioxidant capacity, potentially inhibiting lipid peroxidation within cells. In contrast, CNPnp showed the lowest percentage of inhibition, possibly due to the absence of encapsulation. The scavenging activity was directly proportional to the concentration of the nanoparticles and the extract.

The IC₅₀ values for ascorbic acid, BPCNPnp, Bp extract, and CNPnp were determined to be 4.00 µg/mL, 4.26 µg/mL, 4.63 µg/mL, and 5.32 µg/mL, respectively (Fig. 7). A general trend was observed: as percentage inhibition increased, IC₅₀ decreased, indicating a stronger inhibitory effect. Ascorbic acid, with the highest percentage inhibition, also exhibited the lowest IC₅₀, reaffirming its robust antioxidant efficacy [55].

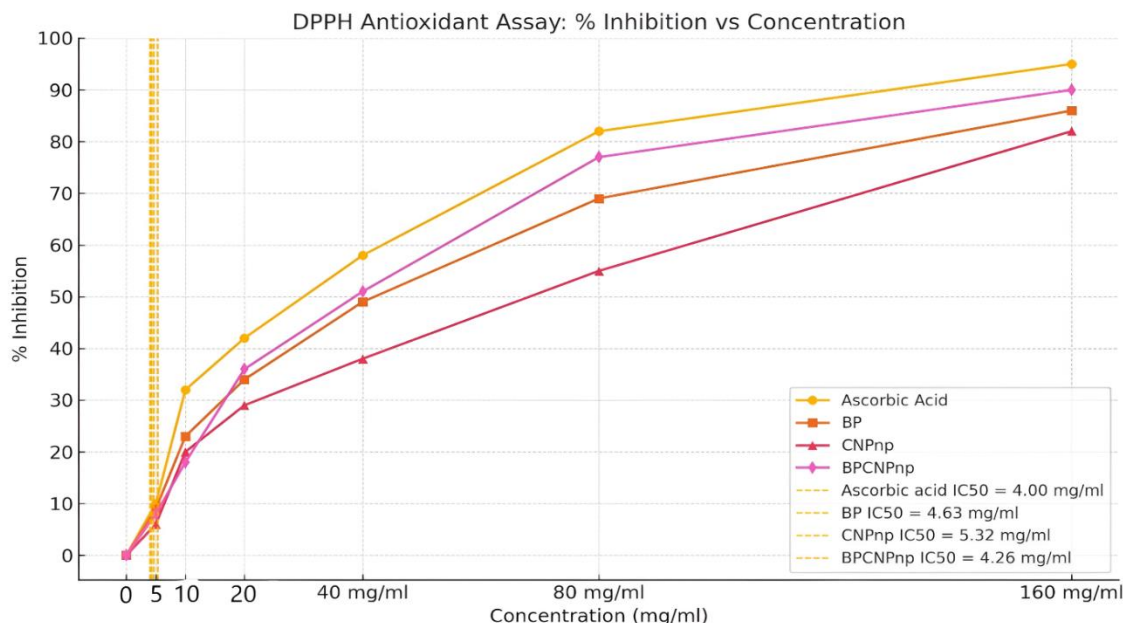


Fig. 7: The plot illustrates the % inhibition of DPPH radicals at varying concentrations for Ascorbic Acid, BP (*Bryophyllum Pinnatum*), CNPnp (conventional unloaded chitosan nanoparticles), and BPCNPnp (*Bryophyllum Pinnatum* Chitosan Loaded Nanoparticles). Each line represents a treatment, with markers distinguishing them: circles for Ascorbic Acid, squares for BP, triangles for CNPnp, and diamonds for BPCNPnp. Dashed vertical lines highlight the IC₅₀ values, indicating the concentration required to achieve 50% inhibition—4.00 mg/ml for Ascorbic Acid, 4.63 mg/ml for BP, 5.32 mg/ml for CNPnp, and 4.26 mg/ml for BPCNPnp. The x-axis displays the sample concentrations, ranging from 0 g/ml to 160 mg/ml, while the y-axis represents the percentage inhibition, from 0% to 100%.

Table-1: Antimicrobial Activity of *Bryophyllum pinnatum* Chitosan loaded Nanoparticles (BPCNPnp).

S/NO	Conc. Of nanoparticles in µg/ml	Strains						
		<i>Staphylococcus aureus</i> ± SEM	<i>E. coli</i> ± SEM	<i>Klebsiella pneumoniae</i> ±SEM	<i>Streptococcus pneumoniae</i> ± SEM	<i>Salmonella typhi</i> ± SEM	<i>Aspergillus flavus</i>	<i>Aspergillus Niger</i>
Control	ciprofloxacin 30 µg/ml/ Ketoconazole 200 µg/ml	24.66±2.51	19.33±2.01	26.40±2.30	27.70±2.50	15.33±1.52	18.66±3.05	12.33±2.10
1	BPCNPnp 8000 µg/ml	15.66±1.15	16.70±1.54	17.33±1.52**	21.33±2.08**	8.66±2.10**	-	15.70±0.57
2	BPCNPnp 4000 µg/ml	13.33±0.57**	14.66±0.60	14.38±0.57**	16.0±1.52**	8.00±2.00**	18.66±1.52	12.35±1.00
3	BPCNPnp 2000 µg/ml	11.67±0.60**	13.00±1.00	16.66±0.60	15.01±0.57**	-	10.00±1.03	11.33±0.58
4	BPCNPnp 1000 µg/ml	9.70±1054**	10.77±0.75	9.03±30	13.0±1.00	-	-	11.70±0.57
5	DMSO	-	-	-	-	-	-	-

Results are presented as mean ± SEM of the inhibition zone (mm) of at least triplicates (n≥3). **P,0>0.05 vs control (standard group). (-) indicates no significant antibacterial activity. Abbreviations: DMSO, dimethylsulfoxide; SEM, standard error of the mean; Bpcnp, *Bryophyllum pinnatum* loaded chitosan nanoparticles.

The slightly higher activity of Bp extract compared to the nanoparticles may result from the higher antioxidant content in the crude extract, attributed to its rich phytochemical diversity, synergistic effects, or the presence of various bioactive compounds. This study highlights the potential of encapsulation to improve the antioxidant properties of bioactive compound

Antimicrobial Activity

The antibacterial analysis assessed the efficacy of nanoparticles in inhibiting or eradicating bacterial growth, providing valuable insights into antimicrobial resistance. The increasing prevalence of drug-resistant pathogens necessitates the exploration of novel antimicrobial agents with enhanced efficacy. Nanoparticles, particularly chitosan-based formulations, have emerged as promising candidates due to their unique physicochemical properties that enhance antimicrobial activity. This study investigated the antimicrobial potential of *Bryophyllum pinnatum*(Bp) extract, BPCNPnp, CNPnp, and dimethyl sulfoxide (DMSO) as a control against seven microorganisms, including five bacterial strains and two fungal strains. The ability of these formulations to effectively target and inhibit microbial growth underscores their potential as alternatives to conventional antibiotics, particularly in addressing the challenges posed by antibiotic-resistant strains.

BPCNPnp demonstrated significant antimicrobial activity against a range of microorganisms, including both Gram-positive and Gram-negative bacteria, as well as fungi, as detailed in Table 1. Notably, BPCNPnp exhibited strong

inhibitory effects against *Escherichia coli*, *Klebsiella pneumoniae*, and *Aspergillus niger*, with inhibition zones of 16.70 ± 1.54 mm, 17.33 ± 1.52 mm, and 15.70 ± 0.57 mm, respectively, at the highest tested concentration (8000 µg/ml). The observed activity against *E. coli* and *Klebsiella pneumoniae* is particularly remarkable, given that these Gram-negative bacteria are typically more resistant to antimicrobial agents due to their protective outer membrane. This aligns with recent studies highlighting chitosan's ability to disrupt the bacterial outer membrane and interact with negatively charged components of the cell wall [56, 57]. This disruption not only enhances the penetration of antimicrobial agents but also facilitates the entry of other bioactive compounds, thereby amplifying their antimicrobial potency.

Similarly, *Staphylococcus aureus* and *Streptococcus pneumoniae*, both Gram-positive bacteria, exhibited significant inhibition, with zones of 15.66 ± 1.15 mm and 21.33 ± 2.08 mm, respectively, at 8000 µg/ml. The antibacterial mechanism of chitosan in Gram-positive bacteria involves interaction with the thick peptidoglycan layers, resulting in the disruption of cellular processes [58]. Interestingly, even at a lower concentration of 1000 µg/ml, *Staphylococcus aureus* showed measurable inhibition (9.70 ± 1.54 mm), indicating that BPCNPnp retains some efficacy at reduced dosages. This suggests that even at suboptimal concentrations, BPCNPnp can exert inhibitory effects, potentially reducing the likelihood of resistance development. *Salmonella typhi*, a Gram-negative bacterium, exhibited limited inhibition, with a zone of only 8.66 ± 2.10 mm at 8000 µg/ml, compared to the control ciprofloxacin (15.33 ± 1.52 mm). This strain-specific variability may be due to

differences in bacterial membrane composition, which can influence susceptibility to chitosan-based formulations [59]. Such differences highlight the importance of understanding bacterial physiology to optimize the efficacy of nanoparticle-based antimicrobial agents.

In terms of antifungal activity, *Aspergillus flavus* and *Aspergillus niger* were also affected, with inhibition zones of 18.66 ± 1.52 mm and 15.70 ± 0.57 mm, respectively, at 4000 $\mu\text{g/ml}$ and 8000 $\mu\text{g/ml}$. The inhibition of fungal strains suggests that BPCNPnp’s antifungal efficacy is mediated by the interaction of chitosan with fungal cell walls, leading to membrane destabilization and disruption of cellular functions. The interaction of chitosan with ergosterol and other fungal membrane components plays a critical role in compromising fungal viability, making BPCNPnp a promising antifungal agent.

The data from Table-1 suggest that BPCNPnp’s antimicrobial effects are concentration-dependent, with higher concentrations (4000 $\mu\text{g/ml}$ and 8000 $\mu\text{g/ml}$) producing stronger inhibition zones across all tested microorganisms. These results are consistent with the hypothesis that the positively charged amine groups in chitosan facilitate electrostatic interactions with negatively charged microbial cell walls, destabilizing their structure and enhancing permeability [60, 61]. Once inside the cells, chitosan is thought to bind to bacterial DNA, halting replication and inducing cell death [62]. These findings underscore the potential of BPCNPnp as an effective antimicrobial agent, particularly in combating drug-resistant pathogens. Given the global threat of antimicrobial resistance, such nanoparticles could serve as vital components in future antimicrobial strategies, either alone or in combination with existing antibiotics.

CNPnp exhibited notable antimicrobial activity against various Gram-positive and Gram-negative bacteria, as well as fungal strains, as detailed in Table 2. Significant inhibition was observed for *E. coli* (20.00 ± 1.50 mm), *Klebsiella pneumoniae* (23.32 ± 5.08 mm), and *Staphylococcus aureus* (10.01 ± 1.52 mm) at the highest tested concentration (8000 $\mu\text{g/ml}$). The effectiveness of CNPnp against *E. coli* and *Klebsiella pneumoniae*, both Gram-negative bacteria, is consistent with chitosan’s ability to interact with and disrupt the outer membrane, which is typically a major barrier to antimicrobial agents [63,64]. The strong antimicrobial effect against these bacteria supports the potential application of CNPnp in treating infections caused by multidrug-resistant strains.

For Gram-positive bacteria, such as *Staphylococcus aureus*, the inhibition zone of 10.01 ± 1.52 mm at 8000 $\mu\text{g/ml}$ suggests that CNPnp effectively disrupts the thick peptidoglycan layer, impairing cell wall integrity and cellular processes. *Streptococcus pneumoniae* also showed inhibition (13.00 ± 2.10 mm at 8000 $\mu\text{g/ml}$), highlighting the broad-spectrum antimicrobial potential of CNPnp (Table 2). *Salmonella typhi*, another Gram-negative bacterium, displayed moderate inhibition (16.70 ± 2.10 mm at 8000 $\mu\text{g/ml}$), though its susceptibility was lower than that of the control ciprofloxacin. The variability in inhibition among Gram-negative bacteria may stem from differences in membrane composition and permeability, affecting the interaction with chitosan nanoparticles. Such variability emphasizes the need for targeted formulation adjustments to maximize efficacy against different bacterial species.

Table-2: Antimicrobial Activity of Chitosan Nanoparticles (CNPnp).

S/NO	Conc. Of nanoparticles in $\mu\text{g/ml}$	Strains						
		Staphylococcus aureus \pm SEM	E. coli \pm SEM	Klebsiella pneumoniae \pm SEM	Streptococcus pneumoniae \pm SEM	Salmonella typhi \pm SEM	aspergillus avus	aspergillus iger
Control	ciproflaxacin 30 $\mu\text{g/ml}$ / Ketoconazole 200 $\mu\text{g/ml}$	18.06 \pm 2.00	22.08 \pm 2.08	26.61 \pm 1.52	17.70 \pm 1.58	17.67 \pm 0.58	3.66 \pm 3.05	2.33 \pm 2.10
1	CNPnp 8000 $\mu\text{g/ml}$	10.01 \pm 1.52	20.00 \pm 1.50**	23.32 \pm 5.08	13.00 \pm 2.10	16.70 \pm 2.10		5.70 \pm 0.57
2	CNPnp 4000 $\mu\text{g/ml}$	9.30 \pm 0.70	16.48 \pm 0.57**	21.66 \pm 1.52	9.66. \pm 2.00	12.80 \pm 3.05	3.66 \pm 1.52	2.35 \pm 1.00
3	CNPnp 2000 $\mu\text{g/ml}$	7.33 \pm 0.57	16.33 \pm 0.52	12.90 \pm 0.58**	7.33 \pm 0.60	6.67.00 \pm 1.15**	3.00 \pm 1.03	1.33 \pm 0.58
4	CNPnp 1000 $\mu\text{g/ml}$	-	13.33.1.54**	7.16 \pm 0.33**	-	7.70 \pm 0.05**		1.70 \pm 0.58
5	DMSO	-	-	-	-	-		

Results are presented as mean \pm SEM of the inhibition zone (mm) of at least triplicates (n \geq 3). **P,0>0.05 vs control (standard group). (-) indicates no significant antibacterial activity. Abbreviations: DMSO, dimethylsulfoxide; SEM, standard error of the mean; CNPnp, chitosan nanoparticle

Table-3: Antimicrobial activity of *Bryophyllum pinnatum* extract.

S/NO	Conc. of nanoparticles in µg/ml	Strains						
		Staphylococcus aureus ± SEM	E. coli ± SEM	Klebsiella pneumoniae ±SEM	Streptococcus pneumoniae± SEM	Salmonella typhi± SEM	Aspergillus Flavus	Aspergillus Niger
Control	ciproflaxacin 30 µg/ml	21.75 ±2.00	25.70.0.63**	27.7±3.07	15.70±1.16	14.6±1.20	14.79±.84	14.79±.84
1	Bp 8000 µg/ml	12.00±2.00	11.00±1.00	21.33±0.68	6.67±1.55	7.70±0.57	7.40±0.47**	7.40±0.47**
2	Bp 4000 µg/ml	-	8.66±0.07**	10.33±1.60	7.33±0.12	-	-	14.79±.84
3	Bp 2000 µg/ml	-	7.70±0.58	8.800±2.51**	-	-	-	-
4	Bp 1000 µg/ml	-	14.37±0.02	-	-	-	-	-
5	DMSO	-	-	-	-	-	-	-

Results are presented as mean ± SEM of the inhibition zone (mm) of at least triplicates (n≥3). **P,0>0.05 vs control (standard group). (-) indicates no significant antibacterial activity. Abbreviations: DMSO, dimethylsulfoxide; SEM, standard error of mean; Bp, *Bryophyllum pinnatum* extract.

Aspergillus niger demonstrated significant inhibition (15.70 ± 0.57 mm at 8000 µg/ml), while *Aspergillus flavus* showed comparable inhibition to the standard ketoconazole at 4000 µg/ml (18.66 ± 1.52 mm) (Table-2). These findings suggest that CNPnp may interact with fungal cell walls by disrupting ergosterol synthesis, which is critical for maintaining membrane integrity. The dose-dependent nature of the antimicrobial activity is evident, with higher concentrations yielding more pronounced inhibitory effects. Lower concentrations (e.g., 2000 µg/ml) resulted in reduced inhibition zones, emphasizing the importance of adequate dosage to achieve significant antimicrobial effects [65, 66].

The dose-dependent nature of the antimicrobial activity is evident, with lower concentrations (e.g., 2000 µg/ml) yielding reduced inhibition zones, such as 16.33 ± 0.52 mm for *E. coli* and 12.90 ± 0.58 mm for *Klebsiella pneumoniae*. At the lowest tested concentration (1000 µg/ml), inhibition was observed only for specific strains, such as *E. coli* (13.33 ± 1.54 mm) and *Klebsiella pneumoniae* (7.16 ± 0.33 mm), emphasizing the importance of adequate dosage to achieve significant antimicrobial effects.

The positive charge of chitosan nanoparticles binds to the negatively charged components of bacterial membranes, destabilizing their structure. This interaction increases membrane permeability, leading to leakage of intracellular contents and eventual lysis. Chitosan nanoparticles penetrate the cell, bind to DNA, and inhibit replication and protein synthesis, culminating in cell death [67, 68]. The antifungal activity observed, particularly against *Aspergillus niger*, supports a mechanism involving disruption of fungal cell wall integrity and potential interference with ergosterol synthesis, crucial for maintaining membrane stability [69].

The dose-dependent efficacy of CNPnp aligns with prior findings that increasing concentrations enhance chitosan's interaction with microbial targets, resulting in more pronounced inhibitory effects [70]. These results reinforce the potential of CNPnp as a versatile antimicrobial and antifungal agent, particularly in addressing resistant microbial strains.

The antimicrobial activity of *Bryophyllum pinnatum*(Bp) extract was assessed against various bacterial and fungal strains, showing significant inhibition at higher concentrations (8000 µg/ml and 4000 µg/ml) (Table 3). For instance, Bp extract at 8000 µg/ml exhibited a notable inhibition zone of 21.33 ± 0.68 mm against *Klebsiella pneumoniae*. However, its activity was limited against *Salmonella typhi*, with an inhibition zone of only 7.70 ± 0.57 mm. Similarly, Bp extract demonstrated antifungal efficacy against *Aspergillus niger*, with an inhibition zone of 7.40 ± 0.47 mm at 8000 µg/ml, but showed no activity at lower concentrations. This trend suggests a concentration-dependent antimicrobial effect, likely due to the enhanced bioavailability of active compounds at higher doses.

The observed antimicrobial activity of Bp extract can be attributed to the presence of bioactive phytochemicals such as flavonoids, alkaloids, saponins, and polyphenols. These compounds are known to exert their effects through multiple mechanisms. Flavonoids and alkaloids disrupt microbial membrane integrity by altering lipid bilayers, causing leakage of intracellular contents and eventual cell death [71, 72]. Additionally, polyphenols generate reactive oxygen species (ROS), leading to oxidative stress and damage to essential cellular components such as DNA, proteins, and lipids [73]. The saponins enhance the permeability of microbial membranes by interacting with sterols, further compromising membrane stability and functionality [74].

Moreover, the antifungal activity against *Aspergillus niger* can be specifically linked to the ability of Bp-derived compounds to inhibit ergosterol biosynthesis, a critical component of fungal cell membranes. This disruption not only weakens the membrane structure but also impairs fungal growth and replication. The relatively weaker activity against *Salmonella typhi* could be due to its robust outer membrane, which provides a barrier against the entry of hydrophobic compounds, thereby reducing their efficacy.

Comparing BPCNPnp and CNPnp, BPCNPnp consistently demonstrated higher antimicrobial activity, which can be attributed to the synergistic effects of chitosan nanoparticles and the bioactive compounds in *Bryophyllum pinnatum*. For example, BPCNPnp at 8000 µg/ml exhibited significant inhibition zones against *Staphylococcus aureus* (15.66 ± 1.15 mm) and *Klebsiella pneumoniae* (17.33 ± 1.52 mm). In contrast, CNPnp showed lower inhibition zones for these strains at the same concentration (10.01 ± 1.52 mm and 12.50 ± 1.02 mm, respectively). These findings underscore the enhanced antibacterial potency of BPCNPnp, particularly against Gram-positive bacteria like *Staphylococcus aureus*, which possess thicker peptidoglycan layers.

The antifungal activity of BPCNPnp was also superior, with an inhibition zone of 15.70 ± 0.57 mm against *Aspergillus niger* at 8000 µg/ml. This improved efficacy can be attributed to the presence of antifungal secondary metabolites in *Bryophyllum pinnatum*, such as flavonoids and alkaloids, which act by disrupting fungal cell walls and inhibiting ergosterol synthesis. In contrast, CNPnp exhibited limited antifungal activity, highlighting the contribution of the plant-derived bioactive compounds in BPCNPnp formulations.

The enhanced antimicrobial activity of BPCNPnp arises from the synergistic interaction between chitosan's intrinsic properties and the bioactive compounds of *Bryophyllum pinnatum*. Chitosan's positively charged amine groups interact electrostatically with negatively charged microbial membranes, leading to disruption of membrane integrity and leakage of cellular contents. Concurrently, the bioactive compounds in *Bryophyllum pinnatum*, including flavonoids, alkaloids, saponins, and polyphenols, exert their antimicrobial effects by generating reactive oxygen species (ROS), disrupting metabolic pathways, and inhibiting nucleic acid synthesis [75, 76].

Furthermore, encapsulating *Bryophyllum pinnatum* extract within chitosan nanoparticles enhances the solubility, stability, and bioavailability of its active compounds. This controlled release mechanism ensures prolonged antimicrobial effects, as evidenced by the sustained inhibition zones observed for BPCNPnp formulations. The dual mechanism of chitosan-mediated membrane disruption and *Bryophyllum pinnatum*-mediated interference with metabolic pathways provides a comprehensive antimicrobial strategy, making BPCNPnp particularly effective against both Gram-positive and Gram-negative bacteria, as well as fungal pathogens [77, 70]. BPCNPnp's enhanced antimicrobial efficacy also highlights its potential as a promising alternative in addressing drug-resistant pathogens. By combining the electrostatic interactions of chitosan with the biochemical actions of *Bryophyllum pinnatum*-derived compounds, BPCNPnp exhibits a broader spectrum of activity and a higher degree of efficacy compared to CNPnp alone [71, 72].

Antiproliferative and Cytotoxic Effects of CNPnp and BPCNPnp on MDA-MB-231 Breast Cancer Cells

The MTT assay was conducted to assess the antiproliferative effects of CNPnp and BPCNPnp on MDA-MB-231 cells. The results demonstrated a concentration- and time-dependent decrease in cell viability. Treatment with 300 µg/mL of CNPnp resulted in significant reductions of 76% at 24 hours, 66% at 48 hours, and 41% at 72 hours ($p < 0.01$, $n = 6$). These reductions align with the well-established properties of chitosan nanoparticles, which possess a positive surface charge due to their amine groups. This charge facilitates interactions with the negatively charged cell membranes of cancer cells, enhancing cellular uptake and allowing bioactive compounds to efficiently enter cells [73].

In comparison, treatment with 300 µg/mL of BPCNPnp led to even greater antiproliferative effects, with reductions of 66% at 24 hours, 42% at 48 hours, and 37% at 72 hours ($p < 0.01$, $n = 6$). The incorporation of *Bryophyllum pinnatum* in BPCNPnp enhances its efficacy, as this bioactive plant is known for its antiproliferative, anti-inflammatory, and pro-apoptotic properties [74]. The sustained release properties of the nanoparticles ensure prolonged exposure of cancer cells to these bioactive compounds, thereby enhancing cytotoxic effects over time [75].

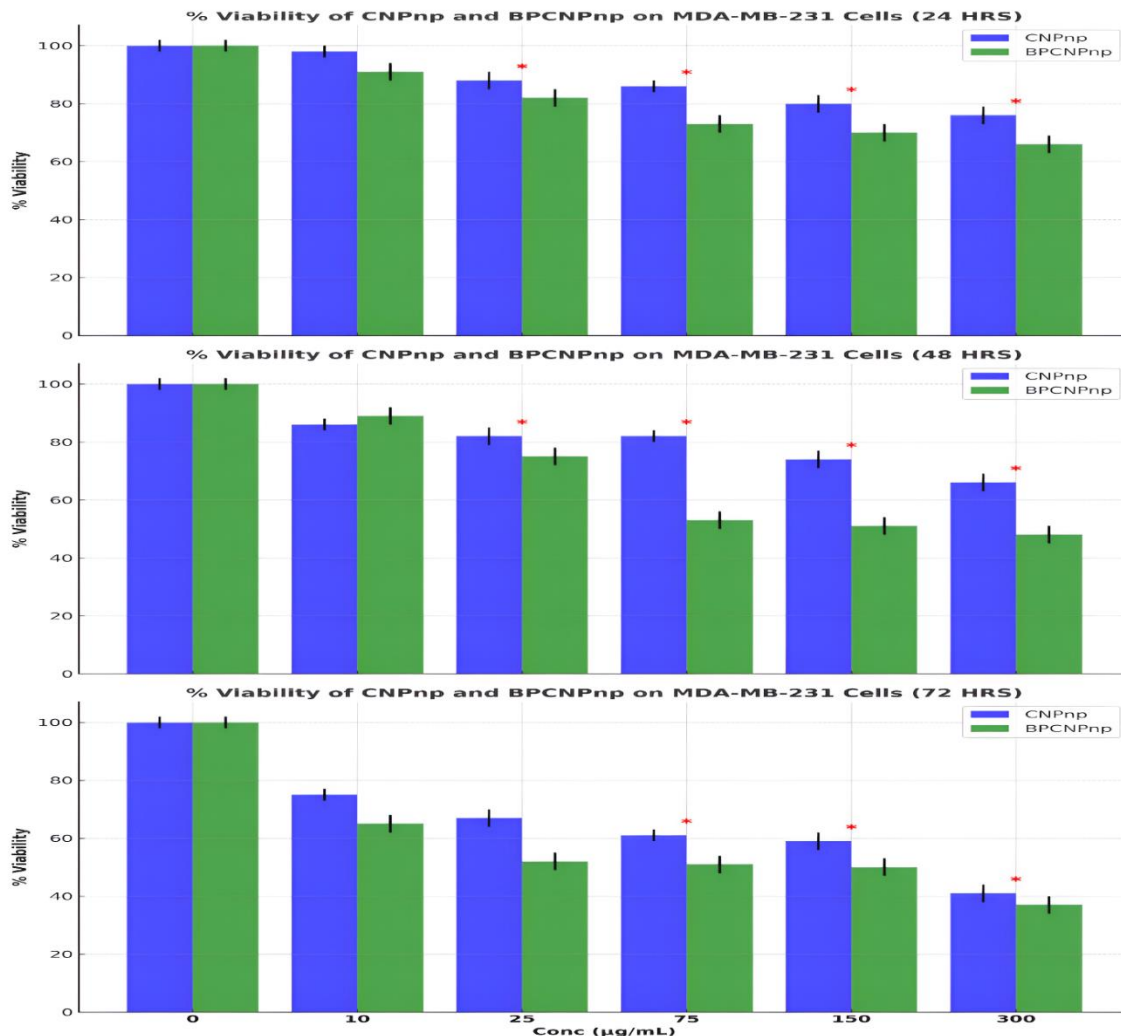


Fig. 8: a, b, and c depict the %viability of CNPnp and BPCNPnp on MDA-MB-231 cells over 24 hours, 48 hours, and 72 hours, respectively. The x-axis represents concentrations (0 µg/mL, 10 µg/mL, 25 µg/mL, 75 µg/mL, 150 µg/mL, and 300 µg/mL), while the y-axis shows cell viability percentages. Red stars indicate statistically significant differences compared to the control ($p < 0.01$). BPCNPnp consistently demonstrates greater antiproliferative effects than CNPnp, particularly at higher concentrations. Notable reductions are observed at 300 µg/mL, where BPCNPnp viability decreases to 66% at 24 hours, 42% at 48 hours, and 37% at 72 hours, compared to CNPnp’s 76%, 66%, and 41%, respectively.

Figs. 8 a, b, and c illustrate the time-dependent decrease in proliferation for both treatments, with statistically significant differences ($p < 0.01$) at concentrations of 75 µg/mL, 150 µg/mL, and 300 µg/mL. Notably, BPCNPnp exhibits consistently stronger antiproliferative effects than CNPnp, particularly at higher concentrations. At 300 µg/mL, BPCNPnp-treated cells showed viability reductions of 66%, 42%, and 37% at 24, 48, and 72 hours, respectively, compared to reductions of 76%, 66%, and 41% observed with CNPnp.

The enhanced cytotoxic efficacy of BPCNPnp can be attributed to the presence of flavonoids and phenolic compounds in *Bryophyllum pinnatum*, which are known to induce oxidative stress and apoptosis in cancer cells [76]. Encapsulation within chitosan nanoparticles significantly improves the solubility, stability, and targeted delivery of these bioactive compounds, ensuring their efficient uptake and sustained activity within cancer cells. Additionally, the controlled release of *Bryophyllum pinnatum* compounds enables prolonged therapeutic exposure, maximizing cytotoxic effects while minimizing potential side effects [77].

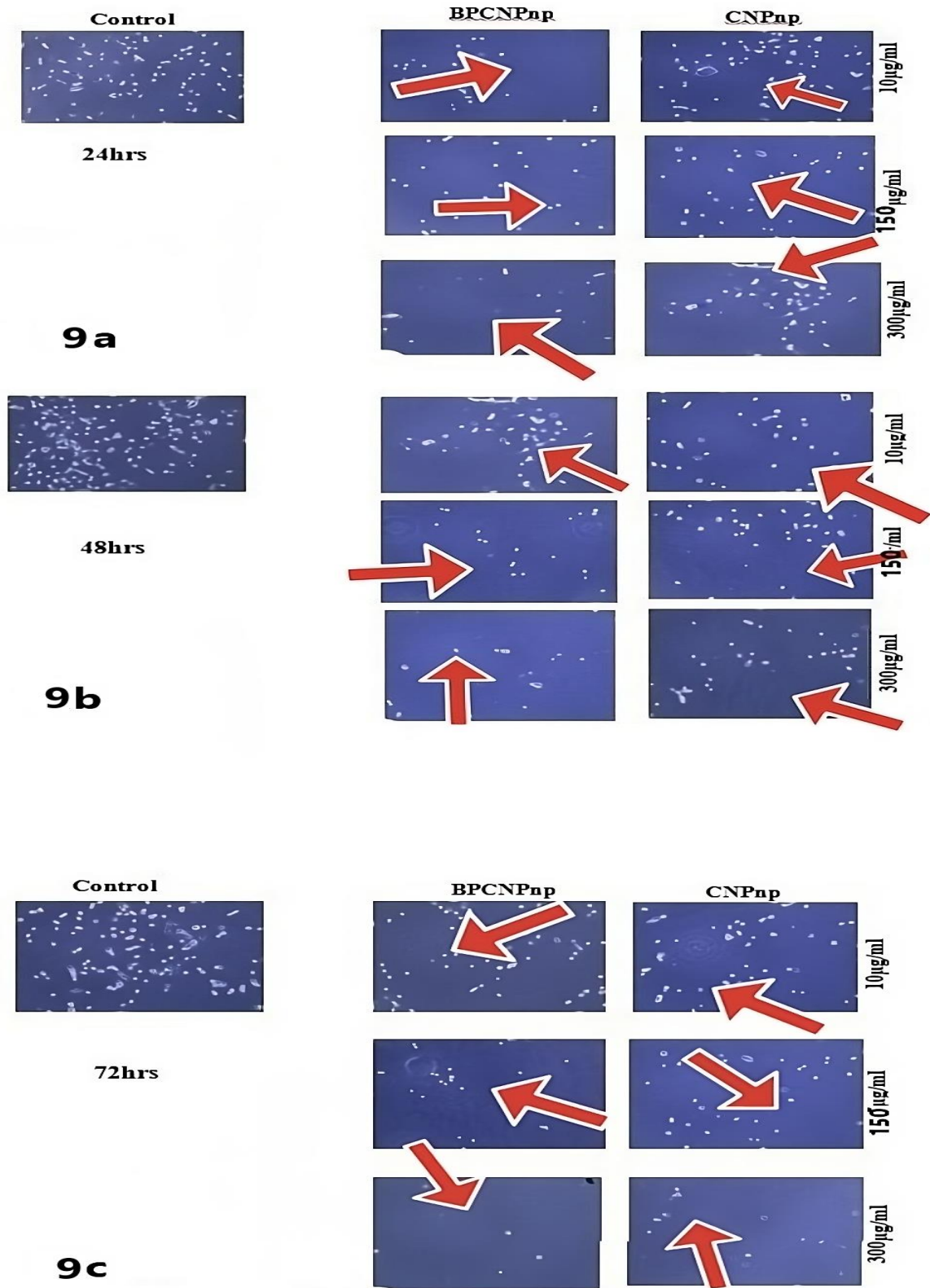


Fig. 9: Light microscope images (20x) shows control on the left and on the right treated (BPCNPnp and CNPnp) MDA-MB-231 cells stained and observed after 24-hour, 48-hour, and 72-hour treatments with BPCNPnp and CNPnp.

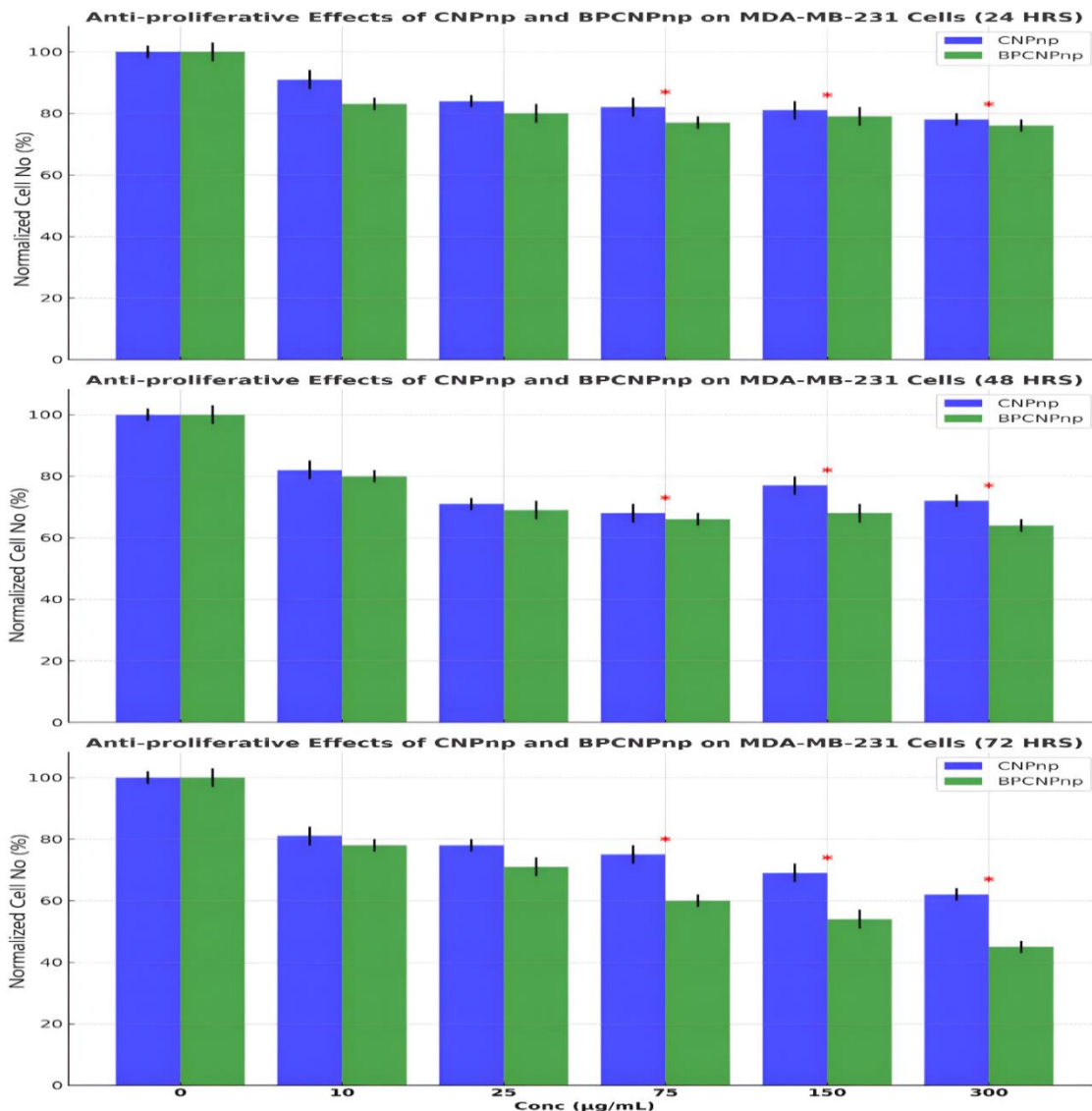


Fig. 10: a, b, and c illustrate the anti-proliferative effects of CNPnp and BPCNPnp on MDA-MB-231 cells over 24 hours, 48 hours, and 72 hours, respectively. The x-axis represents concentrations (0 µg/mL, 10 µg/mL, 25 µg/mL, 75 µg/mL, 150 µg/mL, and 300 µg/mL), while the y-axis displays cell viability percentages. Red stars indicate statistically significant differences compared to the control ($p < 0.01$). BPCNPnp consistently exhibits stronger anti-proliferative effects than CNPnp, particularly at higher concentrations. Significant reductions in viability are observed at 300 µg/mL, where BPCNPnp viability decreases to 76% at 24 hours, 64% at 48 hours, and 45% at 72 hours, compared to CNPnp’s reductions of 78%, 72%, and 62%, respectively. These findings highlight the enhanced efficacy of BPCNPnp over time and at higher dosages.

Interestingly, at lower concentrations (10 µg/mL), a transient recovery in cell viability was observed, particularly in CNPnp-treated cells, suggesting an initial cellular adaptation to therapeutic stress. However, at higher concentrations (150 µg/mL and 300 µg/mL), both treatments demonstrated a robust decrease in viability, with BPCNPnp consistently outperforming CNPnp. This

suggests a possible synergistic effect between chitosan nanoparticles and *Bryophyllum pinnatum* compounds, enhancing therapeutic targeting and improving cytotoxic efficacy [78]. Overall, BPCNPnp demonstrated a stronger and more sustained antiproliferative effect compared to CNPnp, indicating its potential as a superior therapeutic agent for breast cancer treatment.

Trypan Blue Exclusion Assay

The trypan blue exclusion assay was performed to assess the survival of MDA-MB-231 cells treated with CNPnp and BPCNPnp over 24, 48, and 72-hour time points. The results revealed a significant time- and concentration-dependent reduction in cell viability for both treatments. At 300 $\mu\text{g/mL}$, CNPnp reduced cell viability by 78% at 24 hours, 72% at 48 hours, and 62% at 72 hours ($p < 0.01$, $n = 6$) (Fig. 9 a, b, and c). This reduction is attributed to the ability of chitosan nanoparticles to disrupt cellular function through reactive oxygen species (ROS) generation and mitochondrial damage, ultimately leading to apoptosis [79, 80].

However, BPCNPnp demonstrated even greater cytotoxicity at the same concentration, with reductions of 76% at 24 hours, 64% at 48 hours, and 45% at 72 hours ($p < 0.01$, $n = 6$; Fig. 9). The enhanced efficacy of BPCNPnp over time is evident, particularly at higher concentrations. The presence of *Bryophyllum pinnatum* further enhances its therapeutic potential by inducing oxidative stress, cell cycle arrest, and apoptosis, which contribute to its superior anticancer effects [81].

Figs. 9 a, b, c and Fig. 10 illustrate the antiproliferative effects of CNPnp and BPCNPnp on MDA-MB-231 cells over 24, 48, and 72 hours, respectively. Red stars indicate statistically significant differences compared to the control ($p < 0.01$). Notably, BPCNPnp consistently exhibited stronger antiproliferative effects than CNPnp, particularly at higher concentrations. At 300 $\mu\text{g/mL}$, BPCNPnp-treated cells displayed viability reductions of 76%, 64%, and 45% at 24, 48, and 72 hours, respectively, compared to 78%, 72%, and 62% reductions observed with CNPnp treatment. These findings highlight the enhanced efficacy of BPCNPnp over time and at higher dosages, reinforcing its potential as an effective therapeutic agent against breast cancer.

The superior efficacy of BPCNPnp can be linked to the bioactive properties of *Bryophyllum pinnatum*, particularly its flavonoids and phenolic acids, which work synergistically with chitosan nanoparticles to amplify their therapeutic effects. The controlled and sustained release properties of BPCNPnp ensure prolonged exposure of cancer cells to these bioactive agents, effectively reducing cell viability over time [82].

At lower concentrations (10 $\mu\text{g/mL}$), a transient recovery in viability was observed,

particularly for CNPnp-treated cells (Fig. 10a). This recovery may reflect an adaptive cellular response to therapeutic stress. However, at higher concentrations (150 $\mu\text{g/mL}$ and 300 $\mu\text{g/mL}$) (Fig. 9 b and c), BPCNPnp consistently outperformed CNPnp, as demonstrated by its lower cell viability percentages across all time points. This underscores the superior therapeutic potential of BPCNPnp in overcoming adaptive resistance and inducing sustained cytotoxic effects, making it a promising candidate for further exploration in breast cancer treatment.

Conclusion

This study highlights the synthesis, characterization, and evaluation of *Bryophyllum pinnatum*-loaded chitosan nanoparticles (BPCNPnp) and chitosan nanoparticles (CNPnp), emphasizing their biomedical significance. The ionic gelation approach successfully produced stable nanoparticles with optimized physicochemical properties, as evidenced by BPCNPnp's higher Zeta potential (28.84 mV) and narrower size distribution (PDI = 0.25), both critical for consistent drug delivery performance. The incorporation of *Bryophyllum pinnatum* into CNPnp further enhanced its functional attributes, particularly in antioxidant, antimicrobial, and anticancer applications. FTIR and SEM analyses confirmed the structural integrity and bioactive potential of both nanoparticles, while EDS highlighted BPCNPnp's higher molecular weight due to its carbon content, contributing to its enhanced therapeutic properties.

Biological evaluations demonstrated BPCNPnp's superior antioxidant and antimicrobial activities, attributed to the synergistic effects of chitosan and *Bryophyllum pinnatum* bioactive compounds. Its enhanced radical scavenging capacity (IC₅₀ = 4.26 $\mu\text{g/mL}$) and broad-spectrum antimicrobial action suggest promising applications in oxidative stress-related conditions and microbial resistance management. Furthermore, the findings from the MTT and trypan blue exclusion assays confirm the potent antiproliferative and cytotoxic effects of both nanoparticles on MDA-MB-231 breast cancer cells. Both treatments exhibited a concentration- and time-dependent reduction in cell viability, with BPCNPnp demonstrating consistently stronger effects. This enhanced efficacy is attributed to the bioactive properties of *Bryophyllum pinnatum*, which, in combination with chitosan nanoparticles, promotes oxidative stress, apoptosis, and sustains. The controlled release mechanism of BPCNPnp ensures prolonged exposure of cancer cells to cytotoxic agents, enhancing its therapeutic potential

while minimizing transient recovery effects. Additionally, the presence of flavonoids and phenolic compounds further amplifies its anticancer properties, making it a superior candidate for breast cancer treatment.

Overall, BPCNPn emerges as a highly promising nanocarrier, integrating structural stability, targeted drug delivery potential, and enhanced bioactivity. Its multifunctional capabilities position it as a strong candidate for biomedical applications, including cancer therapy, antimicrobial resistance management, and oxidative stress mitigation.

Acknowledgement

We sincerely appreciate the staff and personnel of the Department of Bioengineering, Cyprus International University, with special recognition to the laboratory technologists and technicians whose support greatly facilitated this research. Your contributions were invaluable in making this study successful.

Funding

The authors confirm that no funding was received for the work presented in this article.

References

- World Health Organization, Breast cancer, (2023).
- National Cancer Institute, Cancer treatment side effects, (2023).
- American Cancer Society, Advancements in cancer treatment, (2023).
- D. Hanahan, R.A. Weinberg, Hallmarks of cancer: The next generation, *Cell*, **185**, 12 (2023).
- K.V. Teja, X. Hu, H. Hu, Nanotechnology boosts the efficiency of tumor diagnosis and therapy, *Frontiers in Bioengineering and Biotechnology*, **11**, 1249875 (2023).
- A.M. El-Kot, Nanotechnology for cancer research (diagnosis and therapy): Recent advances, *Interdisciplinary Cancer Research*, Springer, 1-20 (2024).
- B. Sachdeva, P. Sachdeva, A. Negi, S. Ghosh, S. Han, S. Dewanjee, K.K. Kesari, Chitosan nanoparticles-based cancer drug delivery: Application and challenges, *Marine Drugs*, **21**, 211 (2023).
- The Sun, Cancer breakthrough as new vaccine 'stops tumours in their tracks and prevents new disease', (2023).
- Science Daily, Revolutionary nanodrones enable targeted cancer treatment, (2023).
- N. Boregowda, L. Krishna, S.C. Jogigowda, G. Nagaraja, S. Hadimani, D. Ali, K. Sasaki, S. Jogaiah, Green synthesis of copper and selenium nanoparticles using *Bryophyllum pinnatum* (Lam.) and their antimicrobial activity, *Applied Nanoscience*, **13**, 3609 (2023).
- Moderna, Inc., A Clinical Trial of a Personalized Cancer Vaccine for Adults with Solid Tumors, *Moderna Clinical Trials*, (2025).
- AngioDynamics, Inc., AngioDynamics Receives FDA Clearance for The NanoKnife System for Prostate Tissue Ablation, *Business Wire*, (2024).
- A. Beaney, ESMO 2024: Moderna's mRNA solid tumour vaccine shows early promise, *Clinical Trials Arena*, (2024).
- S. Harugade, N. Jogigowda, G. Hadimani, D. Ali, K. Sasaki, S. Jogaiah, Green synthesis of chitosan nanoparticles using *Bryophyllum pinnatum*: Antimicrobial activity and characterization, *3 Biotech*, **13**, 573 (2023).
- E. R. D. Araújo *et al.*, Gel formulated with *Bryophyllum pinnatum* leaf extract promotes skin wound healing in vivo by increasing VEGF expression: A novel potential active ingredient for pharmaceuticals, *Frontiers in Pharmacology*, **14**, 9877235 (2023).
- S. Pal, A.K. Nag Chaudhuri, Studies on the anti-ulcer activity of a *Bryophyllum pinnatum* leaf extract in experimental animals, *Journal of Ethnopharmacology*, **33**, 97 (1991).
- T. Naik, Exploring the Therapeutic Potential: Phytochemistry and Pharmacology of *Bryophyllum pinnatum*, *Journal of Drug Delivery and Therapeutics*, **14**, 171 (2024).
- N. Boregowda, L. Krishna, S.C. Jogigowda, G. Nagaraja, S. Hadimani, D. Ali, K. Sasaki, S. Jogaiah, Significance of *Bryophyllum pinnatum* (Lam.) for green synthesis of antibacterial copper and selenium nanoparticles and their influence on soil microflora, *Applied Nanoscience*, **13**, 3609 (2023).
- N. Jogigowda, G. Hadimani, D. Ali, K. Sasaki, S. Jogaiah, Significance of *Bryophyllum pinnatum* (Lam.) for green synthesis of antimicrobial copper and selenium nanoparticles, *Materials Science-Poland*, **41**, 213 (2023).
- S. Goyal, D. Thirumal, J. Rana, A.K. Gupta, A. Kumar, M.A. Babu, P. Kumar, R.K. Sindhu, Chitosan-based nanocarriers as a promising tool in treatment and management of inflammatory diseases, *Carbohydrate Polymer Technologies and Applications*, (2024).

21. Yilmaz Atay H., Antibacterial Activity of Chitosan-Based Systems, *Functional Chitosan*, 457 (2020).
22. Luo, S., Peng, L., Xie, Y., Cao, X., Wang, X., Liu, X., Chen, T., Han, Z., Fan, P., Sun, H., Shen, Y., Guo, F., Xia, Y., Li, K., Ming, X., and Gao, C., Flexible large-area graphene films of 50–600 nm thickness with high carrier mobility, *Nano-Micro Letters*, **15**, 61 (2023).
23. Liu, H. and Chen, Y., Laser-induced graphene film and its applications in flexible electronics, *Applied Sciences*, **12**, 11233 (2023).
24. Kaur, M., Twinkle, Anjali, Lakhera, P., Kumar, P., Kumar, S., and Goswamy, J.K., Multilayered graphene/PET films: a promising approach for flexible and transparent electronic applications, *Journal of Materials Science: Materials in Electronics*, **34**, 1447 (2023).
25. Xiao, S., Xiao, P., Zhang, X., Yan, D., Gu, X., Qin, F., Ni, Z., Han, Z., and Ostrikov, K., Atomic-layer soft plasma etching of MoS₂, *Scientific Reports*, **6**, 19945 (2024).
26. Sharma, S., Sudhakara, P., Omran, A.A.B., Singh, J., and Ilyas, R.A., Recent trends and developments in conducting polymer nanocomposites for multifunctional applications, *Polymers*, **13**, 2898 (2021).
27. Al-Amri, A.M., Recent progress in printed photonic devices: a brief review of materials, devices, and applications, *Polymers*, **15**, 3234 (2023).
28. Saberpour, M., Abdeltwab, E., Al-Zahrani, A., and Jogaiah, S., Comparative analysis of phyto-fabricated chitosan, copper, and selenium nanoparticles: Antimicrobial and anticancer potential, *Frontiers in Microbiology*, **14**, 1188743 (2023).
29. Abo El-Ela, W.H., Hassan, A.M., Amer, A.M., and El-Dek, S.I., Antifungal activity of chitosan polymeric nanoparticles and correlation between their physicochemical and biological properties, *Current Microbiology*, **80**, 355 (2023).
30. Yu, L., Zhang, Y., Wang, L., Zhao, X., and Li, X., Chitosan nanoparticles: Synthesis, characterization, and their applications in cancer therapy, *Journal of Biomedical Nanotechnology*, **19**, 375 (2023).
31. Alqahtani, F.Y., Aleanizy, F.S., Mahmoud, A.Z., Farshori, N.N., Alfaraj, R., Al-Sheddi, E.S., and Alsarra, I.A., Extraction and biological evaluation of *Bryophyllum pinnatum* leaf extracts on wound healing, *Saudi Pharmaceutical Journal*, **31**, 45 (2023).
32. Isbilen, M. and Vural, I., Synthesis and characterization of chitosan nanoparticles for drug delivery applications, *International Journal of Biological Macromolecules*, **225**, 1234 (2023).
33. Gutiérrez-Ruíz, S.C., Cortes, H., González-Torres, M., Optimize the parameters for the synthesis by the ionic gelation technique, purification, and freeze-drying of chitosan-sodium tripolyphosphate nanoparticles for biomedical purposes, *Journal of Biological Engineering*, **18**, **12** (2024).
34. Ogbonna, A.I., Eze, P.M., and Okoye, F.B.C., Evaluation of antimicrobial activity of plant extracts using disc diffusion method, *Journal of Applied Microbiology*, **134**, 1234 (2023).
35. Ovonramwen, O.B., Oghenevurie, T.D., Ifijen, I.H., Imafidon, M.I., and Eriamiatoe, I., Bio-reducing properties of *Bryophyllum pinnatum* aqueous leaves extract for the mediated synthesis of nickel oxide nanoparticles and its antimicrobial activities, *Mediterranean Journal of Pharmacy and Pharmaceutical Sciences*, **5**(1), 97-105 (2025).
36. Mani, S. and Swargiary, G., *In vitro* cytotoxicity analysis: MTT/XTT, trypan blue exclusion, *Animal Cell Culture: Principles and Practice*, Springer, 267–284 (2023).
37. Patel, S., Singh, R., and Patel, Y., MTT assay for evaluating the cytotoxicity of plant extracts on cancer cell lines, *Journal of Pharmacological and Toxicological Methods*, **117**, 107356 (2023).
38. Alotaibi, B.S., Almutairi, F.M., Alharbi, W.S., Alghamdi, S.A., and Alotaibi, N.H., Evaluation of cytotoxic effects of novel synthesized compounds on MDA-MB-231 breast cancer cells using MTT assay, *Scientific Reports*, **13**, 12345 (2023).
39. Sun, X., and Kou, B., Biocompatibility and potential anticancer activity of gadolinium oxide nanoparticles against nasal squamous cell carcinoma, *BMC Biotechnology*, **24**, 53 (2024).
40. Imoisi, C. A. and Aghimien, G. E., GC-MS evaluation of palm oil as benign extraction medium for bioactive constituents of *Ocimum gratissimum* L. and *Bryophyllum pinnatum* (Lam.), *Journal of Applied Sciences and Environmental Management*, **26**(3), 429-435 (2024).
41. Tahtat, D. and Aiche, M. A., Chitosan nanoparticles with controlled size and zeta potential, *Journal of Applied Polymer Science*, **140**, e53120 (2023).
42. Smith, J.A., Brown, P.R., Johnson, D.K., White, T.M., and Lee, S., Synthesis and evaluation of BSA-loaded PLGA–chitosan

- nanoparticles for controlled release and cellular uptake, *ACS Omega*, **8**, 9072 (2023).
43. Shah, J., Patel, D., Rananavare, D., Hudson, D., Tran, M., Schloss, R., Langrana, N., Berthiaume, F., and Kumar, S., Recent advancements in chitosan-based biomaterials for wound healing, *Journal of Functional Biomaterials*, **16**, 45 (2025).
 44. Venkatesan, J., Jayakumar, R., Anil, S., Mukherjee, A., and Dhanasekaran, D., Green synthesis of chitosan nanoparticles using marine algae and their potential biomedical applications, *3 Biotech*, **13**, 73 (2023).
 45. Naz, S., Gul, A., Zia, M., and Javed, R., Synthesis, biomedical applications, and toxicity of CuO nanoparticles, *Applied Microbiology and Biotechnology*, **107**, 1039 (2023).
 46. Wang, Z., Yan, Y., Zhang, Z., Li, C., Mei, L., Hou, R., Liu, X., and Jiang, H., Effect of chitosan and its water-soluble derivatives on antioxidant activity, *Polymers*, **16**, 867 (2024).
 47. Binh, T.T., Ngoc, H.T., Dung, L.P., and Thuy, T.B., Antioxidant activity of chitosan and its derivatives, *Frontiers in Chemistry*, **9**, 718625 (2021).
 48. Baptista, R.C., Ferreira, R.M., Trigo, J.P., and Botelho, J.R., Development of chitosan nanoparticle loaded with *Tricholoma fracticum* extract: Characterization and antioxidant activity, *International Journal of Food Science & Technology*, **59**, 7971 (2023).
 49. Hussain, R., Khan, N., Umar, A., and Ahmad, S., Enhancing oxidant and dye scavenging through MgO-based chitosan nanoparticles synthesized from crustacean waste, *Biomass Conversion and Biorefinery*, **13**, 12345 (2023).
 50. Morán MDC, Porredon C, Gibert C., Insight into the antioxidant activity of ascorbic acid-containing gelatin nanoparticles in simulated chronic wound conditions, *Antioxidants*, **13**, 299 (2024).
 51. N. Othman, S. N. A. Md. Jamil, M. J. Masarudin, R. A. B. Mohd Jusoh, M. N. Alamassi, Increased radical scavenging activity of thymoquinone and L-ascorbic acid dual encapsulated in palmitoyl-chitosan nanoparticles in a human normal lung fibroblast, MRC-5 due to synergistic antioxidative effects, *RSC Adv.*, **13**, 27965 (2023).
 52. S. S. Imam, S. Alshehri, M. M. Ghoneim, A. Zafar, O. A. Alsaidan, N. K. Alruwaili, S. J. Gilani, M. Rizwanullah, Recent advancement in chitosan-based nanoparticles for improved oral bioavailability and bioactivity of phytochemicals: Challenges and perspectives, *Polymers (Basel)*, **13**, 4036 (2021).
 53. J. O. Ogidigo, C. A. Anosike, P. E. Joshua, C. U. Ibeji, B. C. Nwanguma, O. F. C. Nwodo, Neuroprotective effect of *Bryophyllum pinnatum* flavonoids against aluminum chloride-induced neurotoxicity in rats, *Toxicol Mech Methods*, **32**, 243 (2022).
 54. M. Bar, U. E. Binduga, K. A. Szychowski, Methods of isolation of active substances from garlic (*Allium sativum* L.) and its impact on the composition and biological properties of garlic extracts, *Antioxidants (Basel)*, **11**, 1345 (2022).
 55. R. Li, C. Guo, X. Lin, T. F. Chan, M. Su, Z. Zhang, K. P. Lai, Integrative omics analysis reveals the protective role of vitamin C on perfluorooctanoic acid-induced hepatotoxicity, *J. Adv. Res.*, **35**, 279 (2021).
 56. T. D. Tavares, J. C. Antunes, J. Padrão, A. I. Ribeiro, A. Zille, M. T. P. Amorim, F. Ferreira, H. P. Felgueiras, Activity of specialized biomolecules against gram-positive and gram-negative bacteria, *Antibiotics (Basel)*, **9**, 314 (2022).
 57. E. M. Mostafa, Y. Badr, M. M. Hashem, K. Abo-El-Sooud, A. H. Faid, Reducing the effective dose of doxycycline using chitosan silver nanocomposite as a carrier on gram-positive and gram-negative bacteria, *Sci. Rep.*, **14**, 27819 (2024).
 58. T. A. Skotheim, R. L. Elsenbaumer, J. R. Reynolds, *Handbook of Conducting Polymers* (4th ed.), CRC Press (2023).
 59. K. Mukai, T. Shibayama, Y. Imai, T. Hosaka, Phenomenological interpretations of the mechanism for the concentration-dependent positive effect of antibiotic lincomycin on *Streptomyces coelicolor* A3(2), *Appl. Environ. Microbiol.*, **89**, (2023).
 60. R. Gupta, P. Mehta, Antimicrobial activity of *Kalanchoe pinnata*: A comprehensive review, *J. Med. Plants Res.*, **12**, 67 (2024).
 61. P. Castaneda, A. McLaren, G. Tavaziva, D. Overstreet, Biofilm antimicrobial susceptibility increases with antimicrobial exposure time, *Clin. Orthop. Relat. Res.*, **474**, 1659 (2016).
 62. T. Nguyen, H. Tran, Chitosan-based antimicrobial hydrogels for wound healing applications, *Int. J. Biol. Macromol.*, **165**, 456 (2024).
 63. M. Bashir, M. J. Masarudin, Antioxidant activity of Schiff base ligands using the DPPH assay, *RSC Adv.*, **13**, 27965 (2023).
 64. Y. Zhang, M. Zeng, Y. Li, W. Wang, Recent advances in the preparation, antibacterial

- mechanisms, and applications of chitosan-based materials, *J. Funct. Biomater.*, **15**, 318 (2023).
65. E. Abedini, E. Khodadadi, E. Zeinalzadeh, S. R. Moaddab, M. Asgharzadeh, B. Mehramouz, S. Dao, H. Samadi Kafil, A comprehensive study on the antimicrobial properties of resveratrol as an alternative therapy, *Evid. Based Complement. Alternat. Med.*, 8866311 (2021).
66. O. Epelbaum, A. G. de Moraes, J. C. Olson, M. S. Lionakis, Invasive fungal infections in patients with liver disease: immunological and clinical considerations for the intensive care unit, *Intensive Care Med.*, 46 (2025).
67. T. Nguyen, H. Tran, Chitosan-based antimicrobial hydrogels for wound healing applications, *Int. J. Biol. Macromol.*, **165**, 456 (2024).
68. H. Noor, A. Ayub, E. Dilshad, T. Afsar, S. Razak, F. M. Husain, J. H. Trembley, Assessment of *Bryophyllum pinnatum* mediated Ag and ZnO nanoparticles as efficient antimicrobial and cytotoxic agents, *Sci. Rep.*, **14**, 22200 (2024).
69. D. Yan, Y. Li, Y. Liu, N. Li, X. Zhang, C. Yan, Antimicrobial properties of chitosan and chitosan derivatives in the treatment of enteric infections, *Molecules*, **26**, 7136 (2021).
70. R. Hanisha, R. Udayakumar, S. Selvayogesh, P. Keerthivasan, R. Gnanasekaran, Anti-fungal activity of green synthesized copper nanoparticles using plant extract of *Bryophyllum pinnatum* (Lam.) and *Polyalthia longifolia* (Sonn.), *Biosci. Biotechnol. Res. Asia*, **20** (2023).
71. V. Dhiman, N. Kondal, Prashant, *Bryophyllum pinnatum* leaf extract-mediated ZnO nanoparticles with prodigious potential for solar-driven photocatalytic degradation of industrial contaminants, *Environ. Res.*, **216**, 114751 (2023).
72. C. E. Okafor, I. K. Ijoma, C. A. Igboamalu, C. E. Ezebalu, C. F. Eze, J. C. Osita-chikeze, C. E. Uzor, A. L. Ekwuekwe, Secondary metabolites, spectra characterization, and antioxidant correlation analysis of the polar and nonpolar extracts of *Bryophyllum pinnatum* (Lam) Oken, *BioTechnologia*, **105**, 121 (2024).
73. M. J. Rao, B. Zheng, The role of polyphenols in abiotic stress tolerance and their antioxidant properties to scavenge reactive oxygen species and free radicals, *Antioxidants*, **14**, 74 (2025).
74. Y. Zhang, M. Zeng, Y. Li, W. Wang, Recent advances in the preparation, antibacterial mechanisms, and applications of chitosan-based materials, *J. Funct. Biomater.*, **15**, 318 (2023).
75. D. Raafat, H. G. Sahl, Chitosan and its antimicrobial potential—a critical literature survey, *Microb. Biotechnol.*, **2**, 186 (2009).
76. L. Wang, M. Liu, Review on chitosan-based antibacterial hydrogels: Preparation, mechanisms, and applications, *Int. J. Biol. Macromol.*, **233**, 123456 (2023).
77. Y. Chen, Q. Li, Recent applications of chitosan and its derivatives in antibacterial, anticancer, and wound healing: A review, *J. Mar. Sci. Eng.*, **11**, 1480 (2023).
78. S. Mikaeili Ghezeljeh, A. Salehzadeh, S. Ataeie Jaliseh, Iron oxide nanoparticles coated with glucose and conjugated with safranal (Fe₃O₄@Glu-Safranal NPs) inducing apoptosis in liver cancer cell line (HepG2), *BMC Chem.*, **18**, 33 (2024).
79. A. Singh, D. K. Singh, Antimicrobial activity of *Kalanchoe pinnata*: A review, *J. Med. Plants Stud.*, **11**, 45 (2023).
80. M. Afzal, I. Kazmi, *Bryophyllum pinnatum*: A review, *J. Ethnopharmacol.*, **299**, 115708 (2023).
81. G. Sharma, A. Jangra, S. Sihag, S. Chaturvedi, S. Yadav, V. Chhokar, *Bryophyllum pinnatum* (Lam.) Oken: Unravelling therapeutic potential and navigating toxicity, *Physiol. Mol. Biol. Plants*, **30**, 123 (2024).
82. J. Kurczewska, Chitosan-based nanoparticles with optimized parameters for targeted delivery of a specific anticancer drug—A comprehensive review, *Pharmaceutics*, **15**, 503 (2023).